Title

USE OF EXCESS CARBON-14 DATA TO CALIBRATE MODELS OF STRATOSPHERIC OZONE DEPLETION BY SUPERSONIC TRANSPORTS

Authors

Johnston, Harold S.
Kattenhorn, David.
Written, Gary.

Publication Date

1974-12-01

Submitted to Journal of Geophysical Research

LBL-3548
Preprint

USE OF EXCESS CARBON-14 DATA TO CALIBRATE MODELS OF STRATOSPHERIC OZONE DEPLETION BY SUPERSONIC TRANSPORTS

Harold S. Johnston, David Kattenhorn, and Gary Whitten

December, 1974

Prepared for the U. S. Atomic Energy Commission
under Contract W-7405-ENG-48

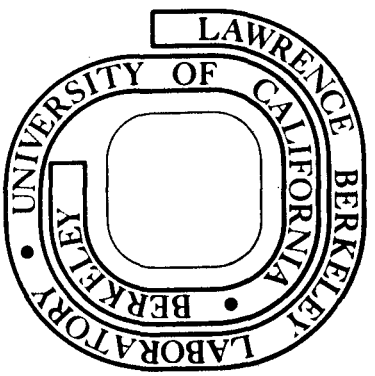

DISCLAIMER

USE OF EXCESS CARBON-14 DATA TO CALIBRATE MODELS OF STRATOSPHERIC OZONE DEPLETION BY SUPERSONIC TRANSPORTS

Harold S. Johnston
Department of Chemistry
University of California
and
David Kattenhorn
Gary Whitten
Inorganic Materials Research Division
Lawrence Berkeley Laboratory
Berkeley, California

ABSTRACT

During 1974, at least seven models of vertical eddy transport and photochemistry have been used to predict the reduction of ozone by nitrogen oxides from supersonic transports. Chang (1974) has shown that these predictions are highly sensitive to the model of vertical eddy diffusion coefficient K_z. In this article, an effort is made to calibrate the one-dimensional K_z functions against quantitative data for the dissipation of excess carbon-14 from the stratosphere during the period 1963-70. The data for excess carbon-14, following the nuclear bomb test series of 1961-62, were published in 1971 and 1972, and these data apparently were not used to derive the various K_z functions. Tables of data are presented in a form that may be useful to others in calibrating two-dimensional and three-dimensional models of stratospheric motion. In checking the one-dimensional models, the direct observations by balloons at 30°N are primarily used, but these data are interpreted as a special hemispherical average (averaging along lines parallel to a standard, sloping tropopause). The carbon-14 data and strontium-90 data differ in many important respects, and it is judged that the carbon-14 data give the better estimate of air motion in the stratosphere. The seven K_z models give predictions that strongly differ from one model to another. The models that give a fairly realistic prediction of carbon-14 distribution and persistence are those with minimum K_z between 15 and 20 km and with increasing K_z from 20 to 50 km. Models with these features, as recalculated by Chang (1974), agree with each other as to ozone reduction by artificial nitrogen oxides from SSTs. These models are used to predict the ozone reduction by SSTs according to Grobecker's (1974) upper-bound projection out to the year 2025. Very large reductions of ozone are indicated - more than a factor of two.

INTRODUCTION

The catalytic reduction of stratospheric ozone by nitrogen oxides from supersonic transport (SST) exhausts was calculated by means of a "box model" and steady-state photochemistry (Johnston, 1971). At that time, the natural background of nitrogen oxides (NO_x) was not known, the quantity of NO_x expected to be emitted by future SST fleets was uncertain, and the photochemical-atmospheric model was primitive, though efficient. By the end of 1974, these uncertainties have been greatly reduced. During 1974, a substantial number of measurements of NO_x in the stratosphere have been reported and are summarized by Hard (1974). Grobecker (1974) has published a projection for the years 1990-2025 of future SST traffic in the stratosphere, and he gave an estimate of the amount of nitrogen oxides that would be emitted in the stratosphere at various altitude bands if future SSTs emit NO_x at the same rate as present ones. Model calculations of the natural stratosphere and the stratosphere as perturbed by SSTs have been made by at least seven different one-dimensional models including vertical eddy transport and extensive O, N, H chemistry (Crutzen, 1974; Chang, 1974; Stewart, 1973; McElroy et al, 1974; Whitten and Turco, 1974; Shimazaki and Ogawa, 1974; Hunten, 1974). Similar calculations have been made including two-dimensional motions by at least three groups (Hesstvedt, 1974; Vupputuri, 1974; and Widhopf and Taylor, 1974). One group has successfully carried out calculations of the SST perturbation problem with a model of three-dimensional atmospheric motions (Cunnold et al, 1974). Model calculations (including only the most recent results reported by each author) of ozone reduction by injection of NO_x at 20 km are given by Figure 1, panel A.

To a considerable extent, these twelve calculations of the SST perturbation (1971-1974) are in agreement; ten out of twelve agree better than a factor of three; but two of them fall far outside this range. Chang (1974) undertook a systematic investigation of the reasons for the discrepancies between the one-dimensional models. He found that Stewart (model 5) had carried out integrations of the SST perturbation for only 18 months, whereas at least 10 years are needed to attain a steady state; this correction brought model 5 into line with ten others. Chang (1974) used his chemical model, his set of boundary conditions, and his computer program to recalculate the predicted SST effect for the seven models involving one-dimensional motions, Figure 1, panel B. The seven vertical eddy diffusion functions, K_z, are given in Figure 2 and in Appendix Table A1. The maximum rate of insertion of nitrogen oxides in Figure 1B corresponds to Grobecker's (1974) upper bound projection for the year 2025.

The curves in Figure 1B differ only with respect to vertical eddy diffusion function, K_z. At low values of NO_x injection rate, there is a spread of a factor of 6 between model 7 and model 12; and at high rates of NO_x injection this spread is a factor of 3. The purpose of this paper is to see if an independent evaluation can be made to assess the accuracy of the seven K_z functions, and to narrow the spread of predictions in Figure 1B.

During and after the period of massive nuclear bomb tests of 1961-62, there was extensive sampling of the stratosphere for radioactive

tracers, including those lodged on solid particles such as strontium-90 and those as gases such as excess carbon-14. There are detailed, zonal-average, contour maps of observed excess carbon-14 in the stratosphere and troposphere every three months (with a few exceptions) from 1955 to 1967 (Telegadas, 1971) and some further data out to 1971 (Telegadas et al, 1972). These data were only recently published and in the form of Health and Safety Laboratory (HASL) Reports of the U.S. Atomic Energy Commission. It appears that none of the modellers of the SST perturbation made detailed, quantitative use of these extensive data. After the end of the test series in December 1962, there was a cloud of carbon-14 covering the northern hemisphere with peak concentration at about 19 or 20 kilometers and with a fairly narrow vertical spread. This case is an appropriate analogy for the SST problem.

In this article, we develop the data in a form that may be useful for testing two and three dimensional models of stratospheric motion, and tables are given in the appendix for this purpose. We take the data at 30°N as primary source for testing the one-dimensional models. However, we carry out an averaging process over the northern hemisphere, both to supplement the direct observations at 30°N and to interpret what a one-dimensional model does. We then take an observed distribution of excess carbon-14 as the initial condition; and we solve the time-dependent, one-dimensional, vertical eddy diffusion equations for subsequent distributions of excess carbon-14, using each of nine K_z functions (the seven used for the SST problem and two more). Numerous

initial and final states were treated. The merit of a given K_z function is judged with respect to how well it predicts the magnitude and shape of the carbon-14 profile as a function of time.

PRIMARY DATA

An example of the observed distribution of excess carbon-14 from the HASL Reports of the U.S. Atomic Energy Commission is shown in Figure 3 (Telegadas, 1971). The units are 10^5 atoms of excess carbon-14 per gram of air and are proportional to mixing ratio or mole fraction. By multiplying by 4.82×10^{-18}, one can convert these units to mixing ratio by volume. The data are from three sources. Balloons were launched at latitudes near 70°N, 30°N, 10°N, and 50°S, and the observed excess carbon-14 is given as numbers on Figure 3. Extensive sampling was done by U-2 aircraft in the stratosphere and by ordinary aircraft in the troposphere, and carbon-14 was measured at numerous ground-level stations. The aircraft and balloon data were used to locate the contour lines on the figure.

The balloon measurements at 30°N for the period January 1963 to January 1966 (Telegadas, 1971) and for November 1970 (Telegadas et al, 1972) are listed in the Appendix, Table A2. From a series of contour maps similar to Figure 3, the mixing ratios were converted to concentration of excess carbon-14 by use of air density data from the Table of Standard Atmospheres. Vertical profiles were drawn at each 10 degrees of latitude, and these profiles were read at each kilometer elevation to give the values in the Appendix, Table A3. There is a

separate chart for January 1963, April 1963, July 1963, October 1963, January 1964, and January 1965. These data were replotted as zonal-average contour maps of excess carbon-14 concentration, five of which are given in Figure 4.

An example of the observed distribution of strontium-90 for April 1963 is shown in Figure 5 (Telegadas, 1967). The units are disintegrations per minute per thousand cubic feet of standard air and are proportional to mixing ratio. The elevations for various values of strontium-90 mixing ratios at 30°N are given in the Appendix, Table A4. From these data, profiles of strontium-90 mixing ratios are readily obtained.

COMPARISON OF CARBON-14 AND STRONTIUM-90 AS TRACERS FOR STRATOSPHERIC AIR MOTIONS

Johnston, Whitten, and Birks (1973) showed that the bulk "residence time" of carbon-14 in the stratosphere (1963-65) was twice as long as that for strontium-90. There must be factors that cause strontium-90 to have a spuriously short residence time, or that cause carbon-14 to have (or appear to have) a spuriously long residence time, or both. It is pointed out below that both of these possibilities can be identified.

Carbon-14 is formed by a nuclear reaction between a neutron and molecular nitrogen. The initial product is probably ^{14}CO, not $^{14}CO_2$. The nuclear bombs of the 1961-62 test series were fired on the surface or in the troposphere, and they were lifted into the stratosphere by thermal buoyancy. Before rising, the fireball cooled to about 6000°K

by emission of radiation and by expansion. The rising fireball was further cooled largely by entrainment of cold air. The gases transported into the stratosphere were subjected to a wide range of temperatures from 6000°K to ambient. Carbon monoxide is burned to carbon dioxide by hot air, and much of the initial ^{14}CO was probably converted to $^{14}CO_2$ in the rising fireball. Unfortunately, the fraction not converted to CO_2 can not be stated with certainty.

If any ^{14}CO survived the high temperatures of the fireball to reach the stratosphere, it would be converted to carbon dioxide by hydroxyl free radicals

$$HO + CO \rightarrow H + CO_2$$

The rate constant for this reaction is 1.4×10^{-13} cm^3 $molecule^{-1}$ sec^{-1} between 200 and 400°K (Garvin and Hampson, 1974). From a mechanism involving O, N, and H chemistry, we calculated the concentration of hydroxyl radicals every hour for 24 hours at 30°N, spring equinox. The 24 hour average concentrations of hydroxyl radicals are given in Table 1. The half-time to convert ^{14}CO to $^{14}CO_2$ is $\ln 2/k\,[HO]_{ave.}$ and these half-times in months are given in Table 1.

The time, location, and approximate yield (megatons, MT) of the 1961-62 nuclear bomb test series are given in Table 2 (recalculated from Seitz et al, 1968). For the reference months of January 1963, January 1964, and January 1965, the elapsed time from the bomb explosions is given. If the fraction α of the carbon-14 entered the stratosphere as ^{14}CO, the remaining fraction after n months is $\alpha \exp(-n/8)$, where 8 months is the average lifetime of CO with respect to oxidation by hydroxyl radicals between 13 and 23 km (Table 1). The yield-weighted residual ^{14}CO at any time is

TABLE 1

THE RATE OF CONVERSION OF CARBON MONOXIDE TO CARBON DIOXIDE IN THE STRATOSPHERE. 24 HOUR AVERAGE VALUES OF HO FREE RADICALS.

Elevation km.	$[HO]_{ave}$ molecules cm^{-3}	CO half-life, months
13	2.9×10^5	6.7
18	3.0×10^5	6.3
23	4.2×10^5	4.5
28	7.5×10^5	2.6

TABLE 2

APPROXIMATE TIMES AND YIELDS (MT) OF NUCLEAR BOMB TESTS IN 1961-62;

MONTHS FROM BOMB EXPLOSION TO VARIOUS LATER TIMES.

Time mo/yr	Location*	MT	months from test until: 1/63	1/64	1/65
9/61	P	9.2	16	28	40
10/61	P	90.5	15	27	39
5/62	T	2	8	20	32
6/62	T	10	7	19	31
7/62	T	2	6	18	30
8/62	P	54	5	17	29
9/62	P	96	4	16	28
10/62	P,T	17	3	15	27
12/62	P	23	1	13	25
	Total:	304			
	maximum residual ^{14}CO		46%	10%	2%

*P, polar, USSR; T, tropical, US or UK. (Seitz et al, 1968)

$$\text{Percent } {}^{14}CO = \frac{100\ \alpha \sum Y_i e^{-n_i/8}}{\sum Y_i}$$

where Y is the yield at the month i.

The maximum residual ^{14}CO occurs if the fraction α is one. By January 1963, the residual ^{14}CO was at most 46 percent; by January 1964, the maximum residual ^{14}CO was 10 percent; and by January 1965, the maximum residual ^{14}CO was 2 percent. It is possible that the carbon-14 data during the year 1963 are distorted to some extent by the conversion of carbon-14-monoxide to carbon-14-dioxide. As can be seen from Table 1, the distortion is altitude dependent, and also it would be season-dependent. In any case, the distortion from this source becomes small after January 1964 and negligible after January 1965. (Combustion of CO in the hot fireball, of course, reduced this effect even more. Conversion of CO to CO_2 in the high-pressure steel tanks between sampling and analysis would also reduce this problem).

Strontium-90 was lodged on solid particles. One immediately suspects that the difference in stratospheric residence times between carbon-14 and strontium-90 is that particulate strontium-90 underwent gravitational settling. However, Telegadas and List (1969) calculated the settling velocity of strontium-90 on the basis of estimates and some measurements of the size of the solid particles containing the radioactive tracer; they concluded that the settling velocity would be slow below 30 km. Their calculations did not consider the possibility that the radioactive particles would ionize the surrounding air and act as condensation nuclei for aqueous sulfuric acid in the

stratosphere. Such enlarged particles would settle faster than the "dry" particles considered by Telegadas and List.

In a purely diffusional process in the vertical dimension, an initial distribution that is narrow and strongly peaked would spread up as well as down. The narrow initial distribution of bomb-debris between 15 and 25 kilometers at 30°N, for example (Figure 4), would spread upwards as the peak concentrations decreased. The profiles of carbon-14 mixing ratios for April 1963, January 1964, and January 1965 are shown in the middle panel of Figure 6. The mixing ratios above 25 km increase as the peak at 21 km decreases with time. The top panel of Figure 6 gives calculated distributions of carbon-14 as a function of time, given the observed distribution of April 1963 as the initial condition. The lowest panel of Figure 6 gives observed mixing-ratio profiles for strontium-90 at 30°N for April 1963, January 1964, and January 1965, the same location and times as for carbon-14 in the middle panel. The strontium-90 behaved qualitatively different from the excess carbon-14. The height of maximum mixing ratio and the full width at half-maximum are the same for the distributions of carbon-14 and strontium-90 in April 1963. In January 1964 and January 1965 the carbon-14 shows strong upward spreading, the mixing ratio at 30 km was greatest for January 1965, was intermediate for January 1964, and was least for April 1963. At the later times, the strontium-90 cloud does not show the upward diffusion displayed by carbon-14. There is no "crossover point". Strontium-90 is less than the initial value at all elevations at the two later times. An explanation of the difference between the observed carbon-14 and

strontium-90 profiles in Figure 6 is that there was a significant gravitational settling of strontium-90 particles.

Another test of the hypothesis that strontium-90 underwent gravitational settling can be made by comparing the mixing ratios of carbon-14 and strontium-90 at fixed locations as a function of time. For example, consider the mixing ratio of both carbon-14 and strontium-90 at 27 km relative to the maximum mixing ratios of each at 21 km, Table 3. The data are based on local balloon measurements, interpolated to 27 km, for April 1963, Tables A2 and A4. The peak mixing ratio at 21 km for ^{90}Sr was 1700 units on April 1963. The peak mixing ratio at 21 km for ^{14}C was 59.4×10^{-16} on April 1963. The mixing ratios at 27 km, relative to the peak value at 21 km, for ^{14}C and ^{90}Sr were the same on April 1963. At later times, however, the relative mixing ratio of ^{90}Sr at 27 km decreased much more rapidly than that for carbon-14. By January 1964, the relative mixing ratio for ^{90}Sr is one third that for ^{14}C, and by January 1965 the ^{90}Sr is only one-tenth the relative value for ^{14}C. It appears very probable that these differences are due to gravitational settling of ^{90}Sr. It thus appears that the carbon-14 data are superior to the strontium-90 data (and probably to other solid, particulate, radioactive tracers) for the purpose of calibrating vertical eddy diffusion functions or two and three-dimensional models of stratospheric motion.

TABLE 3

RELATIVE BEHAVIOR OF ^{14}C AND $^{90}S_R$ MIXING RATIOS AT 27 KM APRIL 1963,

MIXING RATIOS α AT 27 KM.

Date	$\alpha\ ^{14}C$ (units of 10^{-16})	$\frac{\alpha\ C\text{-}14}{59.4}$	$^{90}S_R$ (units*)	$\frac{\alpha\ S_R\text{-}90}{1700}$	$\frac{B}{A}$
		A		B	
4/63	20.2	0.34	600	0.35	1.03
7/63	22.1	0.37	465	0.27	.73
10/63	26.7	0.45	440	0.26	.58
1/64	20.2	0.34	180	0.11	.32
1/65	18.0	0.30	48	0.028	.093

*The units for $^{90}S_R$ mixing ratio are disintegrations per minute per 1000 cubic feet of standard air.

ANALYSIS OF THE CARBON-14 DATA

These data are based on a fairly thin grid so far as global coverage is concerned. There was detailed sampling by aircraft up to 22 km, but there were only widely spaced balloon profiles at higher elevation, compare Figure 3. There were more extensive balloon samples of strontium-90 than carbon-14, especially in the polar region (Telegadas, 1967); these data are useful in assuring the absence of a large reservoir of nuclear debris in the polar stratosphere. Seitz et al (1968) tabulated each explosion of the 1961-62 series (their tables 2-4) with respect to date, yield, and vertical distribution. They pointed out that the observed distributions after the polar tests were quite different from those calculated on the basis of previous experience (1954-58) for tropical tests. If we assume a uniform distribution of nuclear bomb materials over their quoted vertical spread, then only 35 MT out of 304 MT of the large bombs was deposited above 22 km. Thus about 88 percent of the nuclear cloud was deposited in the region that was densely searched by aircraft, and about 12 percent was deposited above the aircraft ceiling. According to the tables by Seitz et al, the portion of nuclear debris above 33 km (the upper limit of the balloon measurements) was 4 MT out of 304 MT. It thus appears that the amount of excess carbon-14 completely outside the range of observations is very small; but the two dimensional distribution of material between 22 and 33 km, which represents about 10 percent of the total is not accurately known.

There is a fairly large error of measurement associated with any one contour map of carbon-14, and no conclusions should be based on minor features. There was a slow transport of carbon-14 from the northern hemisphere to the southern hemisphere, as seen in Table 4. This movement of excess carbon-14 from the northern hemisphere to the southern hemisphere can be treated by a two or a three dimensional model of atmospheric motions. To a one-dimensional model, however, this loss to the southern hemisphere may appear as a faster than real loss to vertical transport.

In spite of the recognized imperfections of the carbon-14 data (a. rate of conversion of ^{14}CO to $^{14}CO_2$, b. incomplete global grid of observations, and c. slow inter-hemisphere transport), these data are valuable for the calibration, verification, or rejection of models of stratospheric motions, especially for the region between 15 and 30 km. Subject to the uncertainties recognized here, the carbon-14 data for the period between January 1963 and December 1970 are used to test nine models of vertical eddy diffusion functions, Table A1.

It was suggested by Seitz et al (1968) that nuclear bomb debris be averaged over the northern hemisphere, not at equal heights above the ground but at equal heights above a sloping tropopause. The sloping lines of constant mixing ratio of carbon-14 are evident in Figure 3, and these lines more or less parallel the tropopause. Of course, there is a time-and-place varying gap in the tropopause. On a year-long basis it is possible to define and use the concept of a "standard tropopause", which we take to be:

TABLE 4

DISTRIBUTION OF CARBON-14 BETWEEN THE NORTHERN HEMISPHERE AND THE SOUTHERN HEMISPHERE FROM JANUARY 1963 TO DECEMBER 1970.

Date	Excess carbon-14 inventory in stratosphere in units of 10^{26} atoms			
	N.H.	S.H.	% N.H.	Ref.
1/63	310	(46)	87	a.
7/63	243	(58)	81	
1/64	203	(52)	80	
7/64	128	(55)	70	
1/65	113	(57)	66	
7/65	92	(59)	61	
1/66	88	(58)	61	
7/66	73	(55)	57	
7/69	45	(41)	52	
12/70	12.8	12.4	51	b.

a. Telegadas, 1971

b. Telegadas et al, 1972

90°N, 8 km	40°N, 13 km
80°N, 9 km	30°N, 14 km
70°N, 10 km	20°N, 15 km
60°N, 11 km	10°N, 16 km
50°N, 12 km	0°, 16 km.

The observed concentrations in Table A3 of the Appendix were averaged by the cosine function to give equal weight to equal area over the three-dimensional globe along lines at equal heights above this "standard tropopause". This average over the northern hemisphere was assigned to 30°N latitude, the latitude of mid-area between the equator and the pole.

This choice of tropopause height is based on the observed slope with latitude of the maximum carbon-14 mixing ratio for a large number of maps, such as Figure 3, during the test moratorium of 1959-1961, and during the period 1963-67 (Telegadas, 1971). Within the somewhat coarse grid of the observations and within a fairly substantial noise factor in the data, the simple linear function (given above) for the average slope of lines of constant mixing ratio seemed as good as any other. It would be desirable to derive this slope from independent meteorological considerations, but such a study is beyond the scope of this article. As will be noted below, most conclusions of this article are based on actual observations by balloons at 30°N, not the hemisphere averages deduced in this way.

The average profiles ascribed to 30°N are listed in Table A5 of the appendix, and they are plotted in Figure 7, for the periods of

January 1963, April 1963, July 1963, October 1963, January 1964, and January 1965. There are insufficient data to support this detailed analysis after 1965. These average-concentrations are converted to average-mixing-ratios at 30°N by dividing by total air concentration. These mixing ratios are listed in Table A6 of the appendix.

The hemisphere-average mixing-ratio profiles (Table A6) are plotted as circles in Figure 8 and the 30°N local profiles (Table A2) are plotted as triangles on the same figure. It can be seen that these two profiles are very nearly the same. There is somewhat more scatter in the locally observed profiles, but the agreement between the two is quite good.

The near-identity of the two sets of profiles in Figure 8 is a matter of interest in itself: the carbon-14 concentrations averaged to 30°N along lines equi-distant above the average, sloping tropopause are very nearly the same as the actual concentrations at 30°N. A one-dimensional, vertical, eddy-diffusion model located at 30°N is, in this sense, a model for the northern hemisphere.

CALIBRATION OF ONE-DIMENSIONAL MODELS AGAINST OBSERVED CARBON-14 DATA.

The profiles of excess carbon-14 for January 1963 were extended to the surface of the earth on the basis of observed carbon-14 in the troposphere, and it was extended from the observed point of highest elevation to 50 km. by a decreasing exponential function. This extended mixing ratio profile was used as the initial condition for

calculations using the various K_z functions. The vertical grid was every kilometer from 0 to 50. The lower boundary condition was that observed at 1 kilometer, which remained constant for several years near $3x10^{-16}$ mixing ratio. The upper boundary condition was that the mixing ratio at 51 km was one-half that at 50 km. The vertical eddy diffusion problem was set up in terms of first-order differencing, which guarantees conservation of mass even with the non-continuous K_z functions of Figure 2. The problem was thus one of 50 simultaneous linear equations with constant coefficients The problem was solved by the Gear method (Hindmarsh, 1972) on the Lawrence Berkeley Laboratories CDC 7600 computer. With the boundary conditions specified, with the initial profile specified, and with use of a given K_z function, it was a simple matter to compute the predicted carbon-14 distribution at any future time. Typically the future profiles were calculated every 3 months for two years and then every year to a total of 10 years. These calculated profiles, for each K_z function, are then compared with the observed ones. This procedure was repeated with the initial distribution taken to be April 1963 instead of January 1963, also July 1963, January 1964 and January 1965. Particular emphasis is given to the calculations that took January 1964 or later as initial condition, since these data presumably are no longer uncertain so far as ^{14}CO and $^{14}CO_2$ are concerned.

These calculations were made for the seven K_z functions shown in Figure 2 and for Brasseur's (1972) "K-max" and "K-min", all of which are listed in Table A1 of the appendix. We have made a large number of

plots of calculated profiles and observed profiles for the nine K_z functions. Three sets of these plots are given by Figures 9, 10, and 11. Each of these plots is of special interest for one reason or another, and each is discussed below.

In Figure 9, the initial profile is that of January 1963 and the predicted profiles are January 1964. This period is of interest in that it represents the case of maximum gradients, and the sharpest initial distribution. There was a substantial change in one year in the northern hemisphere profile, and there was relatively little loss to the southern hemisphere. The different K_z models give drastically different predictions, one relative to another. These differences between models are much larger than uncertainty with respect to ^{14}CO. The predictions of the models will be discussed below.

In Figure 10, the initial profile is that of January 1964 and the observed points are from the balloon measurements directly observed at 30°N in January 1966. Again, there are strong differences in prediction by the 9 models; and the sense of the differences is the same in Figure 10 as in Figure 9.

In Figure 11, the initial profile is that observed locally by balloon in January 1965 and the observed data are those obtained directly by balloon in December 1970. On January 1965, 66 percent of the stratospheric carbon-14 was in the northern hemisphere and 34 percent was in the southern hemisphere, but in December 1970 it was essentially equal in the two hemispheres (Table 4). This transport to the southern hemisphere was

allowed for, as follows: the magnitude of the initial condition was taken to be the average between the northern and southern hemispheres, rather than the actual value in the northern hemisphere. From consideration of Table 4 the actual concentrations of January 1965 were reduced by the factor 0.75. The observed carbon-14 in November 1970 is spread between 20 and 35 km, with a maximum mixing ratio at about 25 km. There were French and Chinese atmospheric tests of nuclear bombs between 1967 and 1970. According to Telegadas et al (1972), the 1967-70 tests inserted radioactive debris between 14 and 18 km in the northern hemisphere and between 15 and 19 km in the southern hemisphere, and they stated that the carbon-14 above 20 km in December 1970 was primarily contributed by the bomb-test series that ended in December 1962.

The predictions of the nine K_z functions are compared with each other and with observed carbon-14 distributions in Figures 9, 10, and 11. Similar comparisons were made with other observed carbon-14 distributions taken as the initial values and with all later observed carbon-14 distributions taken as comparison for predicted versus observed profiles. The pattern shown by Figures 9-11 is confirmed by all of these comparisons.

DISCUSSION

The excess carbon-14 cloud, spread over the northern hemisphere by the atmospheric nuclear bomb test series of 1961-62, appears to provide a useful calibration for theories of stratospheric motions. The observations of carbon-14 provide direct data for large-scale stratospheric sweep-out times in

the region 15 to 25 kilometers.

The vertical eddy-diffusion function, K_z, were derived by the various authors from considerations of: (1) heat flux data; (2) vertical profiles of ozone; (3) vertical profiles of methane; (4) radioactive fall-out from nuclear bomb tests, primarily involving particulate tracers such as strontium-90, tungsten-185, etc. (5) other considerations. It appears that no one made detailed use of the carbon-14 data. Thus this study is an independent test of the models.

The nine models using vertical eddy diffusion constants K_z as a function of height give markedly different predictions, one relative to another, concerning the dissipation of the carbon-14 cloud during the period 1963-70. The relative and absolute prediction made by the nine K_z models is very nearly the same for the three time intervals of Figures 9-11

Figure	Time interval
9	Jan. 1963 - Jan. 1964
10	Jan. 1964 - Jan. 1966
11	Jan. 1965 - Nov. 1970

The model associated with an investigator is often not the only model considered by the investigator. For example, Crutzen has used several other K_z models; and he has used a different, preferred model in recent calculations. Also, Whitten has modified his model. For the present purpose, it is necessary to adhere to these models, even if they do not represent the investigators latest, best judgment, because

these models were used in Chang's (1974) comparative study (Figure 1B) of the effect of model on SST perturbation, and it is desirable to compare predictions of carbon-14 with those for the SSTs. Crutzen's model used here is valuable in showing the effect of K_z constant with height in the stratosphere. Whitten's model is of interest in showing what a large difference in stratospheric sweep-out time is caused by differences in K_z function, Figure 2. Brasseur's "K-min" shows the effect of a very low K_z value high in the stratosphere. McElroy's or Hunten's model shows the effect of a region of low K_z low in the stratosphere. Chang's model shows the effect of a region of low K_z in the mid stratosphere.

The models with large values of K_z at all heights, such as Brasseur's K-max or Whitten's function, sweep excess carbon-14 out of the stratosphere very much faster than that observed. This discrepancy is so large that these models should be discarded, and line 7 should be dropped from Figure 1B.

Chang's model has minimum K_z at 30 km and Brasseur's "K-min" has minimum K_z at 37 km. These models sweep out the region 17 to 21 km at much too fast a rate, but these models build up relatively large mixing ratios near 35 km over a long period of time. Chang's peak mixing ratio at 35 km in Figure 11 agrees with the observed carbon-14, but Brasseur's "K min" retains too much carbon-14 at 35 km.

Except for the discontinuity at 10 km in the troposphere, Crutzen's K_z function is constant with height. It sweeps out the region around 20 km much faster than was observed, and it gives a long-term profile

(Figure 11) of a shape rather different from that observed. A change of the absolute value of K_z can give approximately correct sweep-out times near 20 km, but the shape of the profile is not improved.

Four functions (5, Stewart; 6, McElroy; 8, Shimazaki, and 12, Hunten) are qualitatively similar: large K_z in the troposphere, minimum K_z in the lower stratosphere, and increasing K_z with height from lower to upper stratosphere. They differ largely as to height of tropopause, height of minimum K_z, and magnitude of K_z at the minimum. The relatively small differences in these K_z functions (Figure 2) lead to substantial differences in predicted history of carbon-14 in the stratosphere. The height of Shimazaki's region of small K_z is too low (note the low elevation of peak carbon-14 in Figures 9 and 10), and the average value of his K_z appears to be too large (note the almost totally swept out stratosphere by 1970). Stewart's model gives a fairly good representation of the shape of the carbon-14 profile and very nearly the correct height of maximum carbon-14 in the various comparisons; but the magnitude of his K_z function between 15 and 25 km. appears to be too large, because it always predicts too little carbon-14 in the stratosphere. McElroy's function gives many predictions in approximate agreement with observations (his function is best for the interval January 1964 to January 1965); but the tropopause is about 2 kilometers too high; and this K_z function appears to be too large on the average since it has swept too much carbon-14 out of the stratosphere over the long period of time (Figure 11).

Hunten's model of K_z gives a reasonably correct prediction of the shape, elevation of the maximum, and magnitude of the carbon-14 cloud

for all tested initial and final profiles. It appears to be superior to all the other models tested here. However, even this model somewhat underestimates the persistence of carbon-14 after eight years, Figure 11.

We have explored the effects of introducing small changes in some of the models. The long-term predictions of the K_z functions are very sensitive to small perturbations of the model. The predictions are strongly dependent on both the shape and the magnitude of the K_z function. The long-term, carbon-14, peak-concentration near 20 km (Figure 10, for example) appears to require the qualitative features of McElroy's or Hunten's model, that is, low values between 15 and 20 km and rapidly increasing values above 25 km.

In view of the considerable success of Hunten's model in describing the carbon-14 data, it is of interest to examine the full predictions of his model for a ten year period, taking the initial distribution as of January 1963. In terms of mixing ratios from 0 to 50 km, these predictions are given for January 1964, January 1966, January 1969, and January 1973, that is, 1, 3, 6, and 10 years after the end of the test series, Figure 12. The lower boundary value was taken to be 2.8×10^{-16} at all times. The upper boundary value is that the mixing ratio at 51 km is half that at 50 km (this is very nearly the sense as assuming zero concentration at 51 km). The vertical spread and long persistence of the carbon-14 in the stratosphere are noteworthy. These calculations were repeated with the lower boundary condition set to zero concentration of excess carbon-14, to simulate a rapid rain-out such as would be expected for NO_x in the troposphere. Above 20 km, there was very little

difference after 1 or 3 years and about a 20 percent reduction at 20 km after 6 years. The calculated curve after 10 years is labelled A in Figure 12. There is a noticeable difference in the lower stratosphere but a surprisingly small difference in the middle and upper stratosphere.

There is a strong correlation between the correctness of predicting the carbon-14 profile in Figures 9 and 10 (but not so much so for the long-term case of Figure 11) and the magnitude of the reduction of ozone by the SST perturbation, Figure 1B. In Figures 9 and 10, the best predictions of carbon-14 are made by Hunten, Stewart, and McElroy; and in Figure 1B these predict the three largest reductions of ozone by SSTs. Crutzen, Chang, and Shimazaki give comparable predictions of carbon-14 in Figures 9 and 10, and they give about the same magnitude of ozone depletion, which is about a factor of two less than the Hunten-McElroy-Stewart group. As stated above, Whitten's model gives unrealistic accounts of carbon-14 and it should be dropped from Figure 1B.

It is of interest to consider the reduction of ozone as a function of added NO_x, using Hunten's K_z function, Chang's calculation with Hunten's K_z function (Figure 1B), and Grobecker's (1974) projected injection of NO_x (This projection is an upper bound; it applies if there is no reduction of the NO_x emission index from supersonic transports). Grobecker's projected upper bound NO_x injections at both 17 km (15 to 18) and at 20 km (18 to 21) are given in Table 5. Grobecker's (1974) upper bound NO_x, Chang's (1974) one-dimensional photochemical model with Hunten's (1974) K_z function, give very large reductions of ozone, substantially greater than a factor of two after the year 2010 (Table 5).

TABLE 5

UPPER BOUND PROJECTIONS OF NO_x INSERTION (UNITS OF 10^{12} g NO_2 yr^{-1}) AT 17 KM AND AT 20 KM (GROBECKER, 1974) AND OZONE REDUCTION AS CALCULATED BY CHANG (1974) USING HUNTEN'S K_z FUNCTION (1974)

Year	NO_x insertion		Per cent ozone depletion from NO_x inserted at:		
	17 km	20 km	17 km	20 km	Total
1990	.45	.22	3.0	2.5	5.5
1996	.60	1.3	4.0	13	17
2000	.70	3.0	4.5	23	27
2006	1.0	6.5	6.2	37	33
2010	1.1	9.0	6.7	43	49
2015	1.2	12	7.2	47	54
2020	1.5	20	8.7	52	61
2025	1.6	27	9.2	60	69

ACKNOWLEDGEMENT

This work was supported by the Climatic Impact Assessment Program by means of an interagency agreement between the Department of Transportation and the Atomic Energy Commission through the Inorganic Materials Research Division, Lawrence Berkeley Laboratory.

REFERENCES

Brasseur, G., Stratospheric chemistry, Aeronomica Acta, B41, Institute d' Aeronomie Spatiale de Belgique, Brussels, 1972.

Chang, J. S., Simulations, perturbations, and interpretations, paper presented at the Third CIAP Conference, Cambridge, Mass., Feb. 26 - Mar. 4, 1974.

Crutzen, P., A review of upper atmospheric photochemistry, Can. J. Chem., 52, 1569-1581, 1974.

Cunnold, D. M., F. N. Alyea, N. A. Phillips, and R. G. Prinn, First results of a general circulation model applied to the SST-NO_x problem, Paper presented at a meeting of the AMS/AIAA Second International Conference on the Environmental Impact of Aerospace Operations in the High Atmosphere, San Diego, Calif., July 8-10, 1974.

Garvin, D., and R. F. Hampson, editors. Chemical Kinetics Data Survey, VII, Tables of Rate and Photochemical Data for Modeling of the Stratosphere (Revised), National Bureau of Standards, NBSIR 74-430, 1974.

Grobecker, A. J., Research program for assessment of stratospheric pollution, Acta Astron., 1, 179-224, 1974.

Hard, T. M., Stratospheric trace-gas measurements, Technical Report, Transportation Systems Center, Cambridge, Mass., May 1974.

Hindmarsh, A. C., Gear: Ordinary differential equation system solver, Lawrence Livermore Laboratory Report UCID-30001, Rev. 1, 1972.

Hesstvedt, E., quoted by Chang (1974).

Hunten, D. M., Stratospheric pollution and how it dissipates, submitted to Science, 1974.

Johnston, H. S., Reduction of stratospheric ozone by nitrogen oxide catalysts from supersonic transport exhaust, Science 173, 517-522; Catalytic reduction of stratospheric ozone by nitrogen oxides, UCRL Report No. 20568, 1-106, 1971.

Widhopf, G. F., and T. D. Taylor, Numerical experiments on stratospheric meridianal ozone distributions using parameterized two-dimensional model, Paper presented at the Third Climatic Impact Assessment Conference, Cambridge, Mass., February 26 - March 4, 1974.

Johnston, H. S., G. Whitten, and J. Birks, The effect of nuclear explosions on stratospheric nitric oxide and ozone, J. Geophys. Res. 78, 6107-6135, 1973.

McElroy, M., S. Wofsy, J. Penner, J. McConnell, Atmospheric ozone: Possible impact of stratospheric aviation, J. Atmospheric Sci., 31, 287-300, 1974.

Shimazaki, T., and T. Ogawa, Theoretical models of minor constituents' distributions in the stratosphere and the impacts of the SST exhaust gases, Paper presented at the IAMAP/IAPSO First Special Assemblies, Melbourne, Australia, 1974.

Seitz, H., B. Davidson, J. P. Friend, and H. W. Feeley, Numerical models of transport, diffusion, and fallout of stratospheric radioactive material. Final report on project Streak. Report No. NYO-3654-4. Isotopes - A Teledyne Company, 50 van Buren Avenue, Westwood, New Jersey (May 1968).

Telegadas, K., J. Gray, Jr., R. E. Sowl, and T. E. Ashenfelter, Carbon-14 measurements in the stratosphere from a balloon-borne molecular sieve sampler. Health and Safety Laboratory Report 246, U.S. Atomic Energy Commission, 69-106, 1972.

Telegadas, K., The seasonal stratospheric distribution of Cadmium-109, Plutonium-238, and Strontium-90, Health and Safety Laboratory Report-184, U.S. Atomic Energy Commission, 53-118, 1967.

Telegadas, K., The seasonal stratospheric distribution and inventories of excess carbon-14 from March 1955 to July 1969, Health and Safety Laboratory Report-243, U.S. Atomic Energy Commission, 3-86, 1971.

Telegadas, K., and R. J. List, Are particulate radioactive tracers indicative of stratospheric motions, J. Geophys. Res., 74, 1339-1350, 1969.

Vupputuri, R. K., The role of stratospheric pollutant gases (H_2O, NO_x) in the ozone balance and its implications for the seasonal climate of the stratosphere, Paper presented at the IAMAP/IAPSO First Special Assemblies, Melbourne, Australia, 1974.

Whitten, R. C., and R. P. Turco, The effect of SST emission on the earth's ozone layer, paper presented at the IAMPA/IAPSO First Special Assemblies, Melbourne, Australia, 1974.

TITLES TO FIGURES

1. Calculated percentage reduction of the average global ozone column as a function of the mass of NO_x inserted at 20 km.

   A. Most recent results available for each of twelve different groups.

   B. Seven one-dimensional models of vertical eddy diffusion function K_z were recalculated on a uniform basis by Chang (1974). The upper limit of NO_x insertion is the upper bound projected by Grobecker (1974) for the year 2025.

   The modelers are identified by the number code: (1) Johnston, 1971; (2) Crutzen, 1974; (3) Hesstvedt, 1974, 2D model; (4) Chang, 1974; (5) Stewart, 1974; (6) McElroy et al, 1974; (7) Whitten and Turco, 1974; (8) Shimazaki and Ogawa, 1974; (9) Vupputuri, 1974, 2D model; (10) Widhopf and Taylor, 1974, 2D model; (11) Cunnold et al, 1974, 3D model; (12) Hunten, 1974.

2. Vertical eddy diffusion functions, K_z, for seven one-dimensional modelers:

   - - - - - - - - (2), Crutzen
   —— -- —— -- —— (4), Chang
   — ·· — ·· — ·· — ·· — (5), Stewart
   ——————————— (6), McElroy
   —— · —— · —— · —— · —— (7), Whitten
   —— —— —— (8), Shimazaki
   ——————————— (12), Hunten

3. Relative mixing ratios (10^5 atoms of excess carbon-14 per gram of air) of excess carbon-14 as measured by balloons and U-2 aircraft. The balloon soundings are indicated by numbers on the figure. The data were taken during the period March - May 1963 and are referred to as April 1963. Telegadas, 1971.

4. Concentration of excess carbon-14 (units of 10^3 molecules cm^{-3}) for the indicated times. These zonal-average maps of ^{14}C concentration were derived from mixing ratio maps such as Figure 3.

5. Relative mixing ratios (disintegrations per minute per 1000 cubic feet of standard air) of strontium-90 for April 1963. Telegadas, 1967.

6. Relative mixing ratios at 30°N for carbon-14 and strontium-90 at three times: April 1963, January 1964, and January 1965. The top panel represents the observed carbon-14 distribution on April 1963 and the calculated distribution at the two later times. The middle panel represents three observed profiles of carbon-14; note the upward diffusion of observed carbon-14 in agreement with the theoretical models. The lower panel represents three observed profiles of strontium-90; note the great difference in pattern above 20 km between carbon-14 and strontium-90. The qualitative aspect of the difference between carbon-14 and strontium-90 is that the latter underwent significant gravitational settling over the periods covered here.

7. Northern hemispherical average (see text) concentration of excess carbon-14 as a function of height between January 1963 and January 1965. These averages are ascribed to the geographical average of the northern hemisphere, namely 30°N.

8. Comparison of average (Figure 7) mixing ratios and locally observed (balloon soundings) mixing ratios of excess carbon-14 at 30°N.

   ○, hemispherical average

   △, local observation at 30°N.

9. Comparison of average observed excess carbon-14 on January 1964 with that calculated by nine models of K_z (Figure 2, Table A1) for January 1964. The initial distribution for calculation was the observed distribution for January 1963. Both initial and final conditions correspond to ◯ in Figure 8.

10. Comparison of directly observed excess carbon-14 on January 1966 with that calculated by nine models of K_z for January 1966. The initial distribution for each computation was the observed distribution on January 1964. (In terms of Figure 8: ◯, 1964; △, 1966).

11. Comparison of directly observed carbon-14 mixing ratios on November 1970 with that calculated by nine models of K_z for January 1971. The initial distribution for each computation was the global average, observed distribution on January 1965. According to Telegadas et al (1972), this excess carbon-14 was left over from the 1961-62 test series, and it was not a part of the 1967-70 series of relatively small bombs, which deposited their debris in the stratosphere between 14 and 18 km. (In terms of Figure 8: △, 1965; △, 1970.

12. Calculated spread of excess carbon-14 for ten years on the basis of Hunten's model for K_z. The initial distribution was the observed distribution for January 1963. Curve A is a "rain-out" model after 10 years, with zero excess-carbon-14 at the lower boundary (1 km).

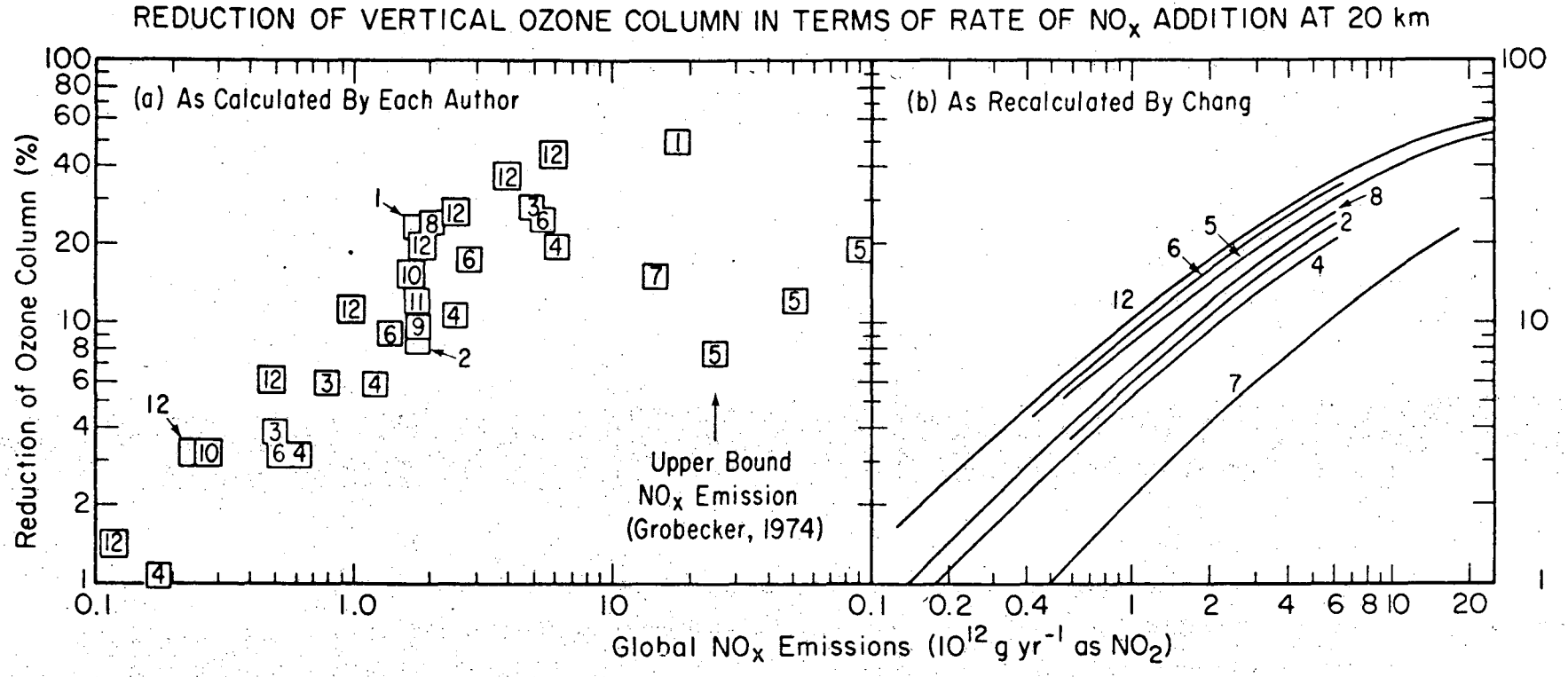

FIGURE 1

XBL-7412-7639

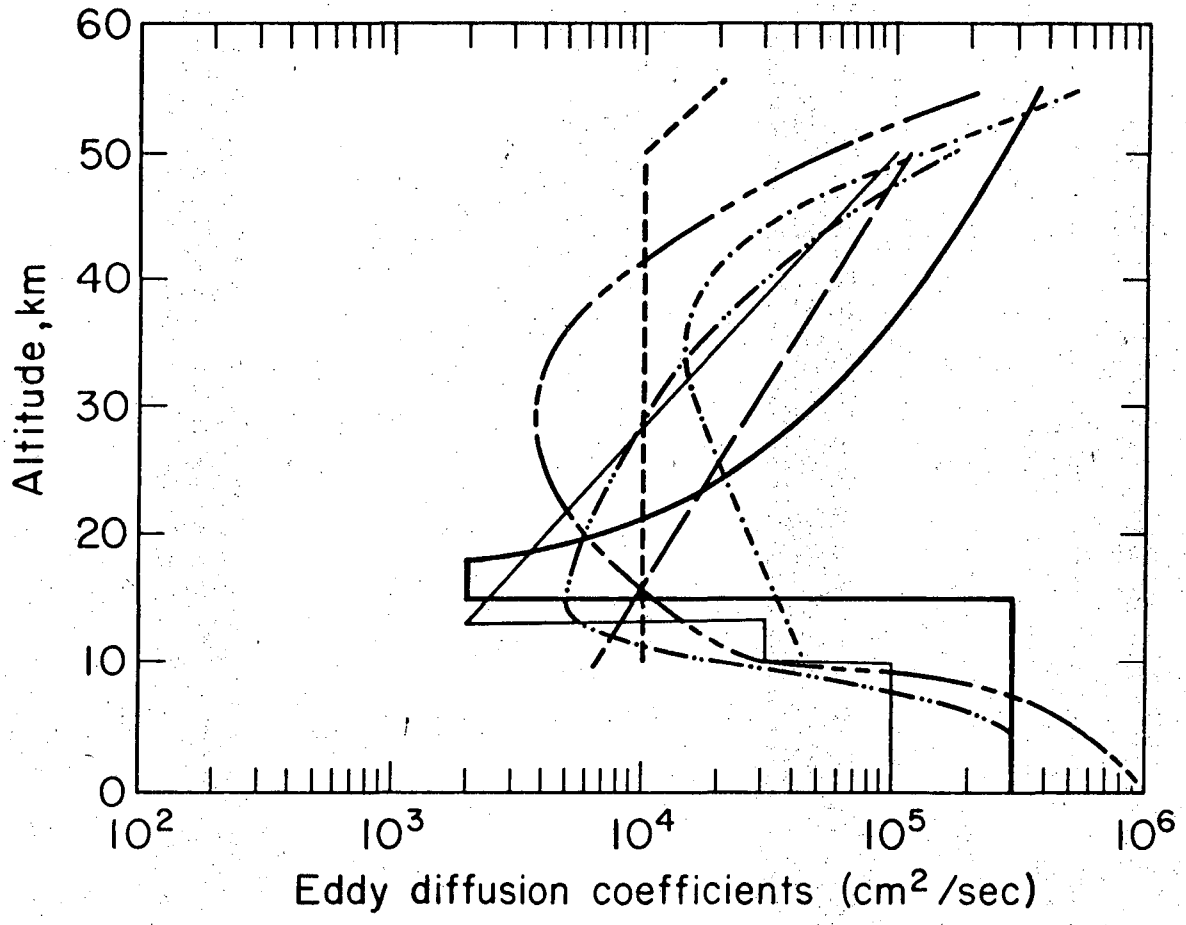

FIGURE 2

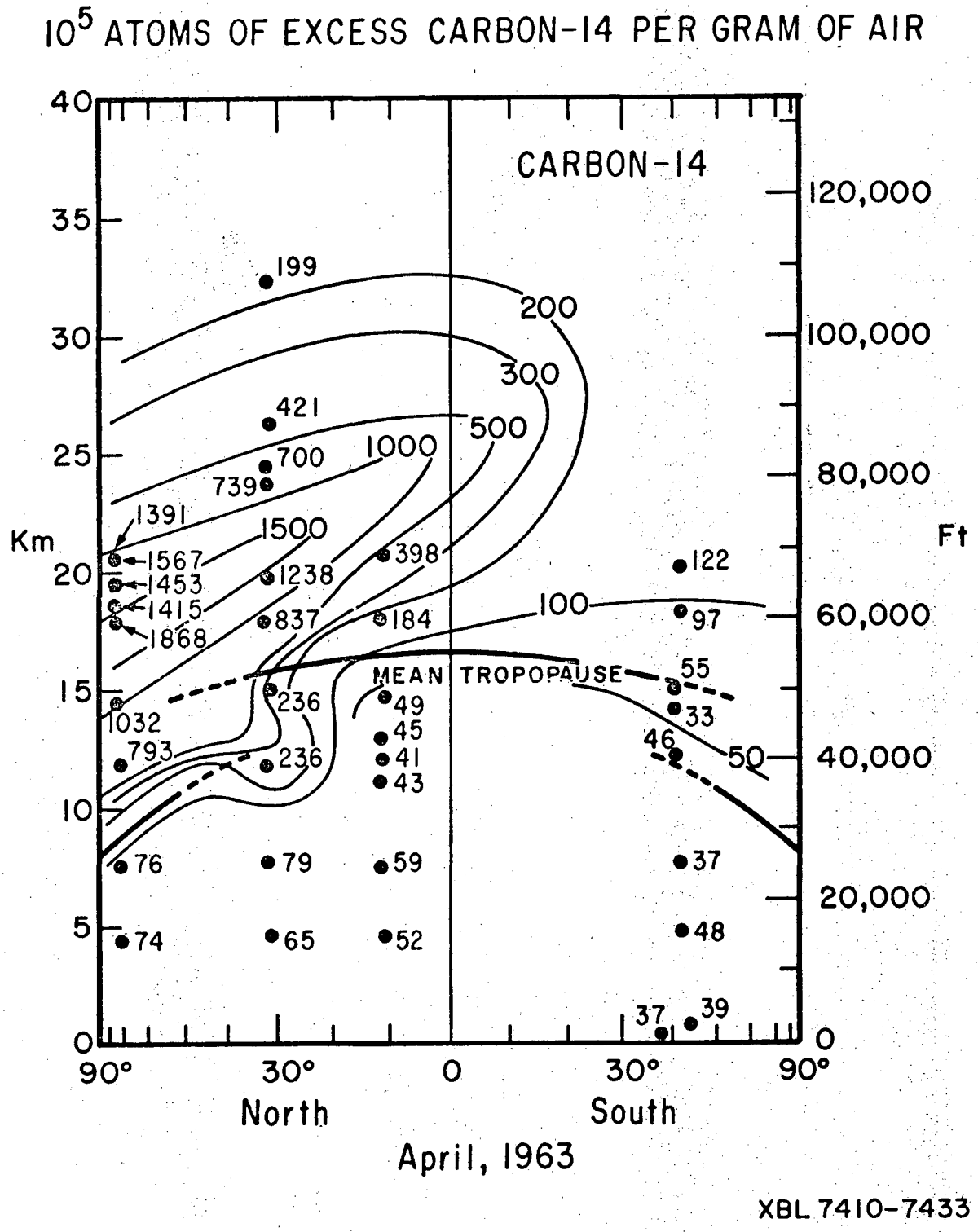
10^5 ATOMS OF EXCESS CARBON-14 PER GRAM OF AIR
CARBON-14
Km
Ft
40
35
30
25
20
15
10
5
0
120,000
100,000
80,000
60,000
40,000
20,000
0
200
300
500
1000
1500
100
50
199
421
700
739
1391
1567
1453
1415
1868
1238
837
398
184
122
97
55
33
46
49
45
41
43
1032
793
236
236
76
79
59
74
65
52
37
48
37
39
MEAN TROPOPAUSE
90°
30°
0
30°
90°
North
South
April, 1963
XBL 7410-7433

FIGURE 3

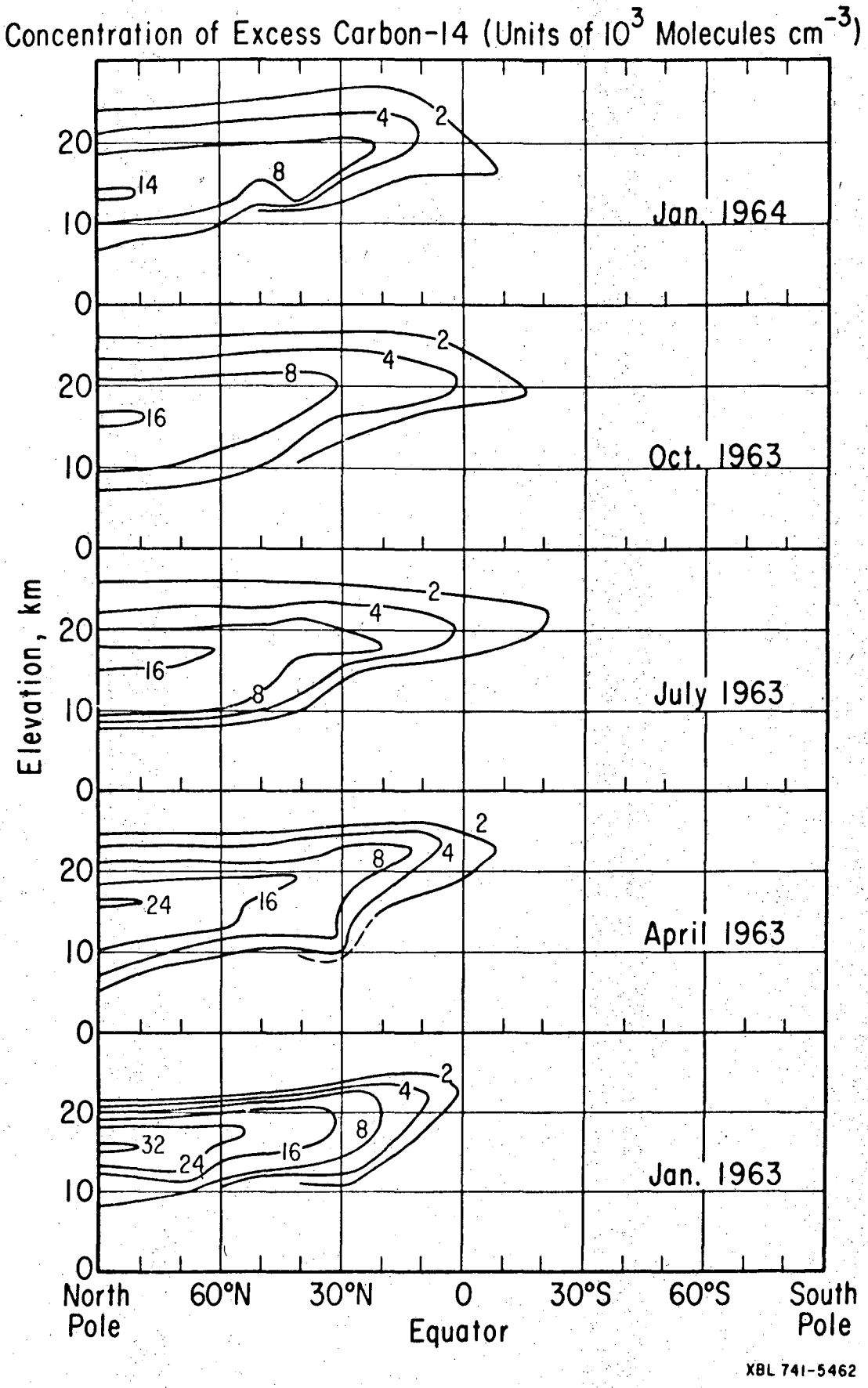

FIGURE 4

STRONTIUM-90

DISINTEGRATIONS PER MINUTE PER 1000 CUBIC FEET OF STANDARD AIR

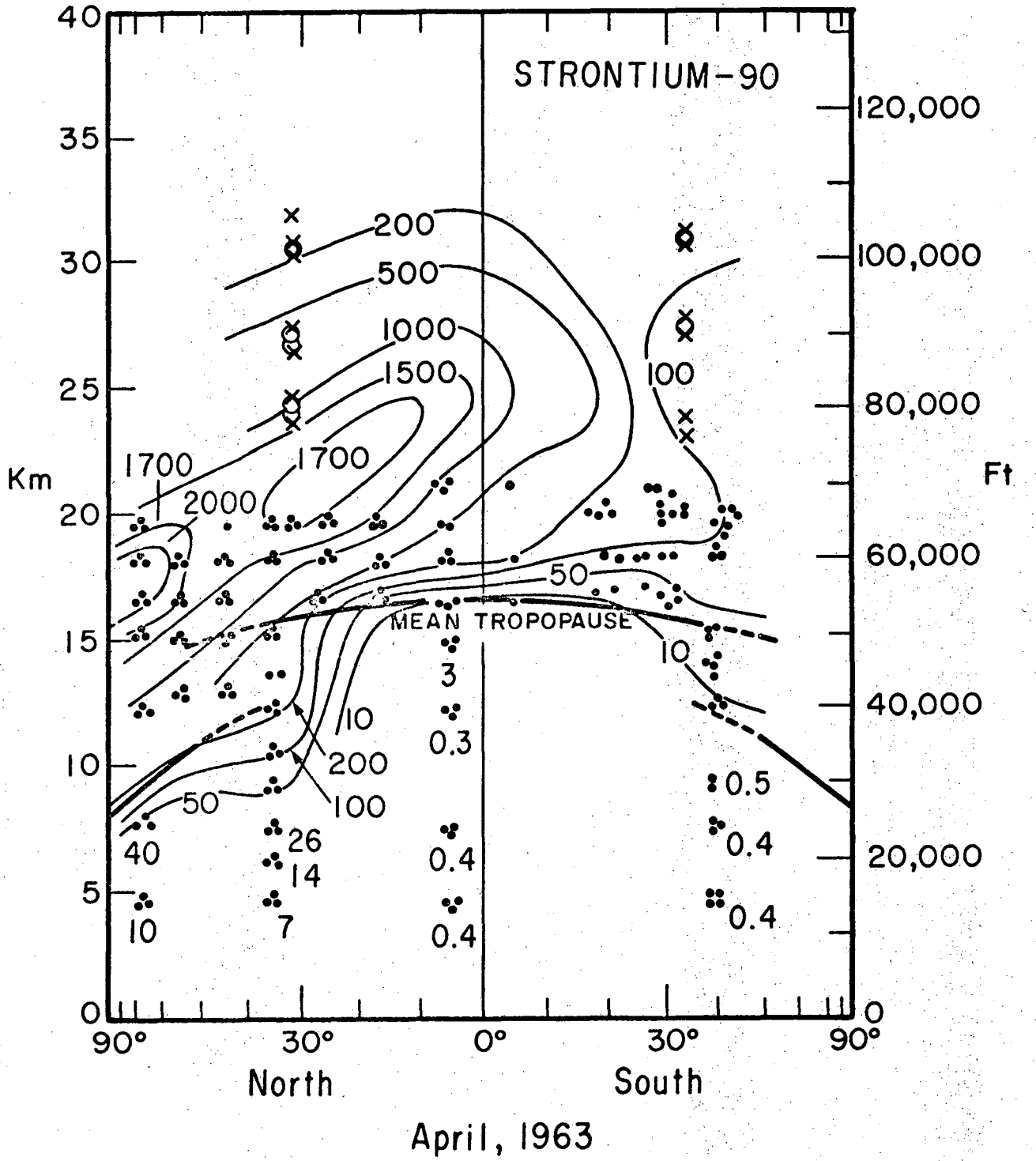

FIGURE 5

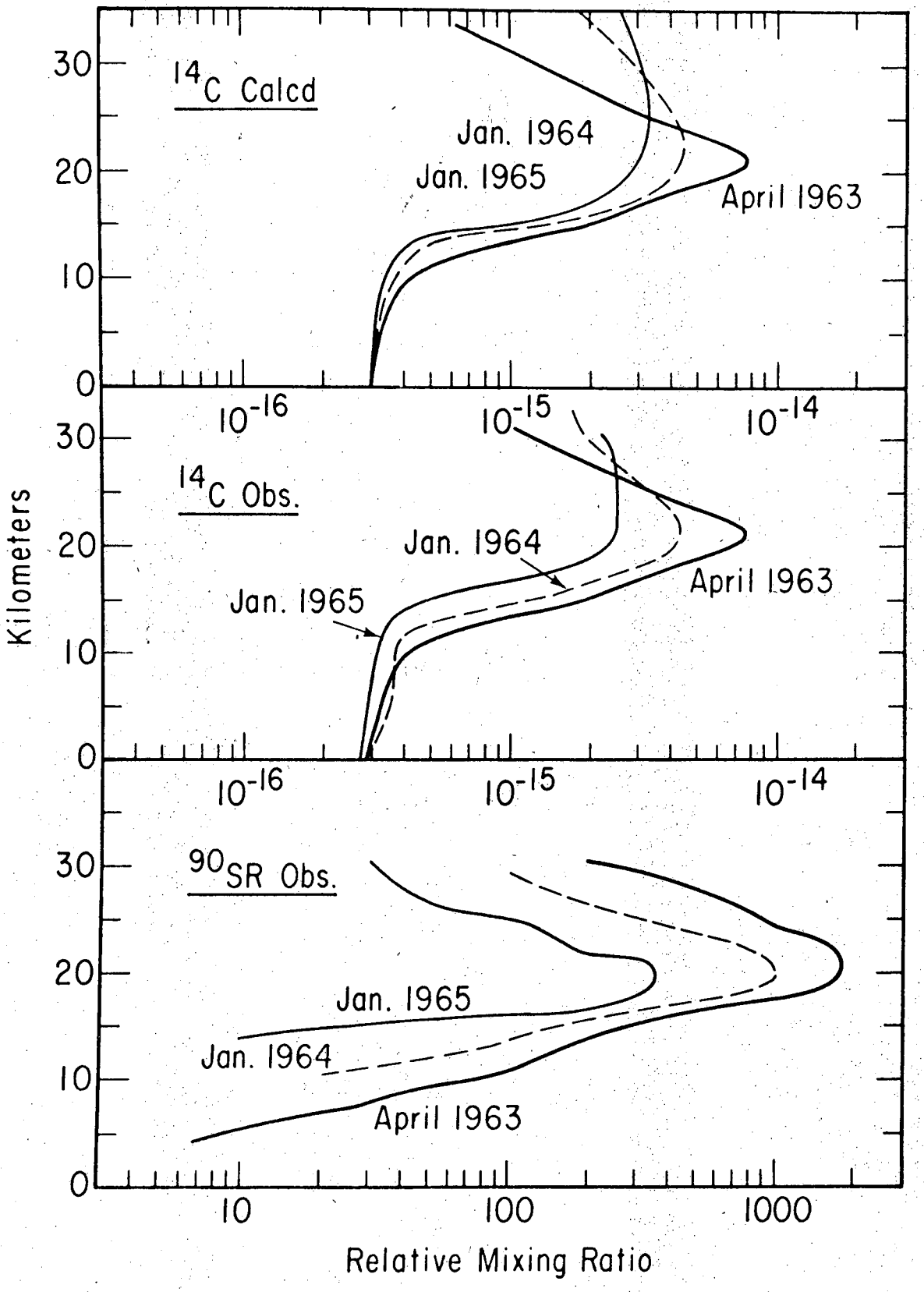

XBL 7410-7435

FIGURE 6

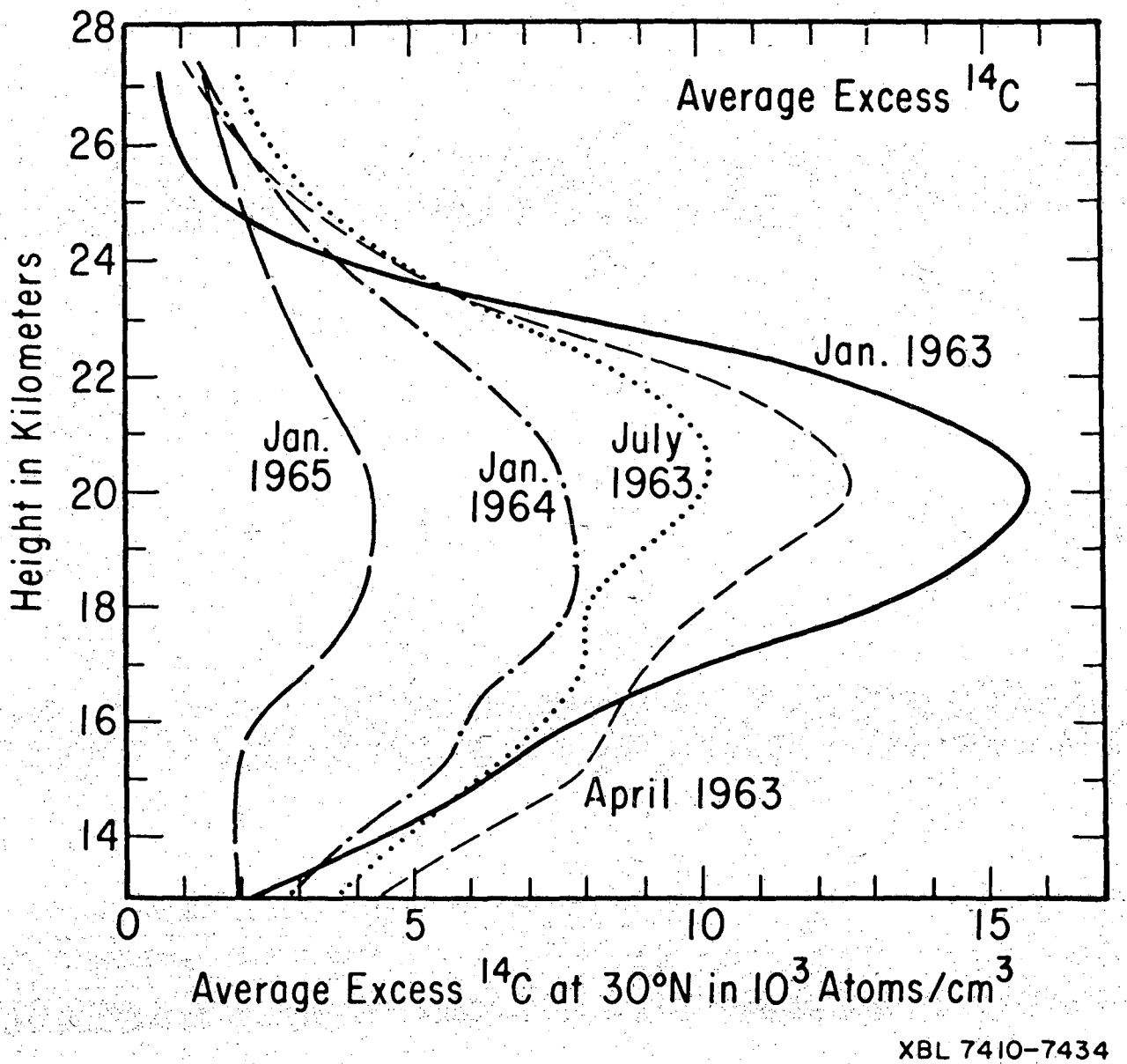
Average Excess ^{14}C
Jan. 1963
July 1963
Jan. 1964
Jan. 1965
April 1963
Height in Kilometers
28
26
24
22
20
18
16
14
0
5
10
15
Average Excess ^{14}C at 30°N in 10^3 Atoms/cm^3
XBL 7410-7434

FIGURE 7

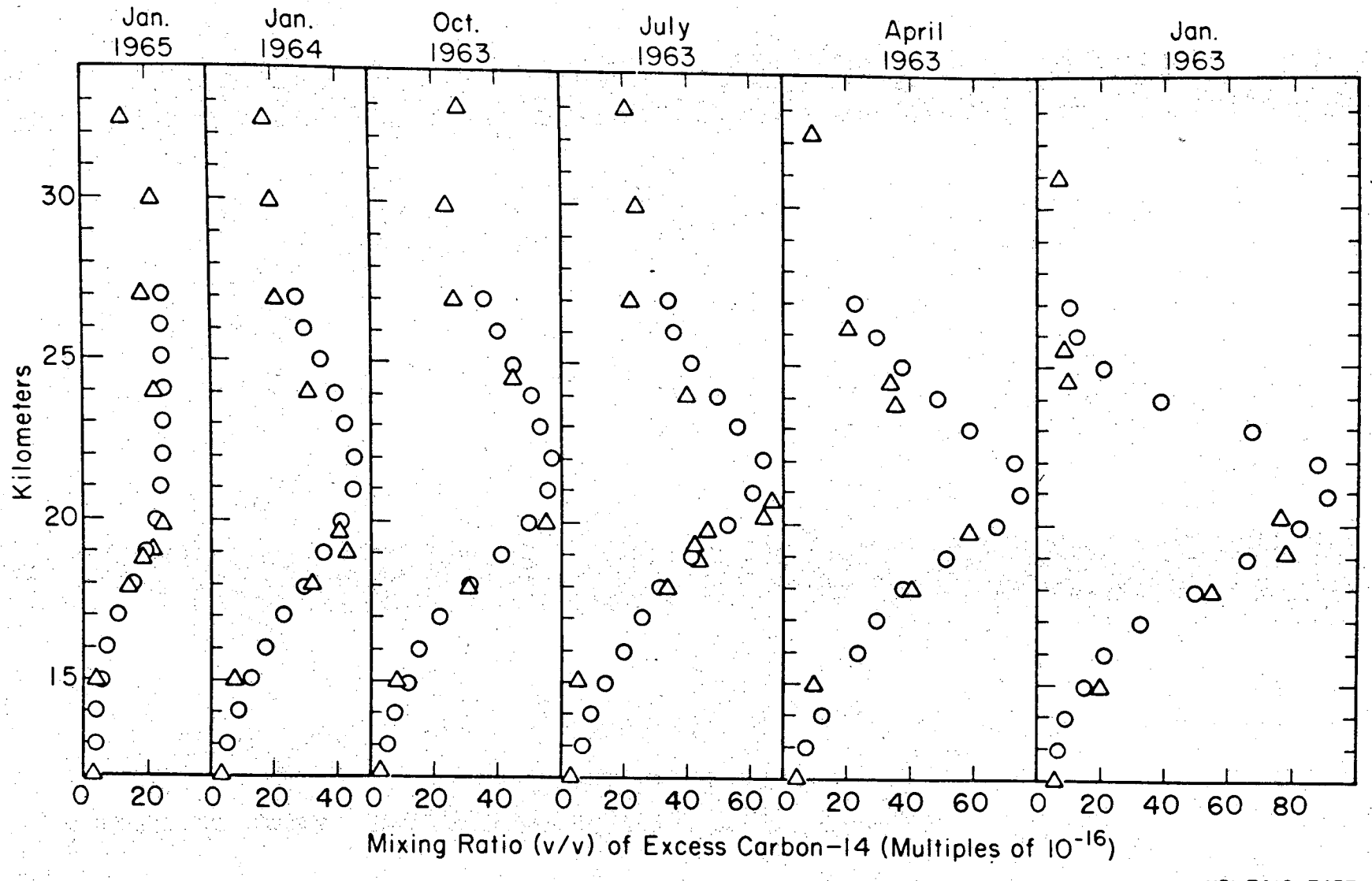

FIGURE 8

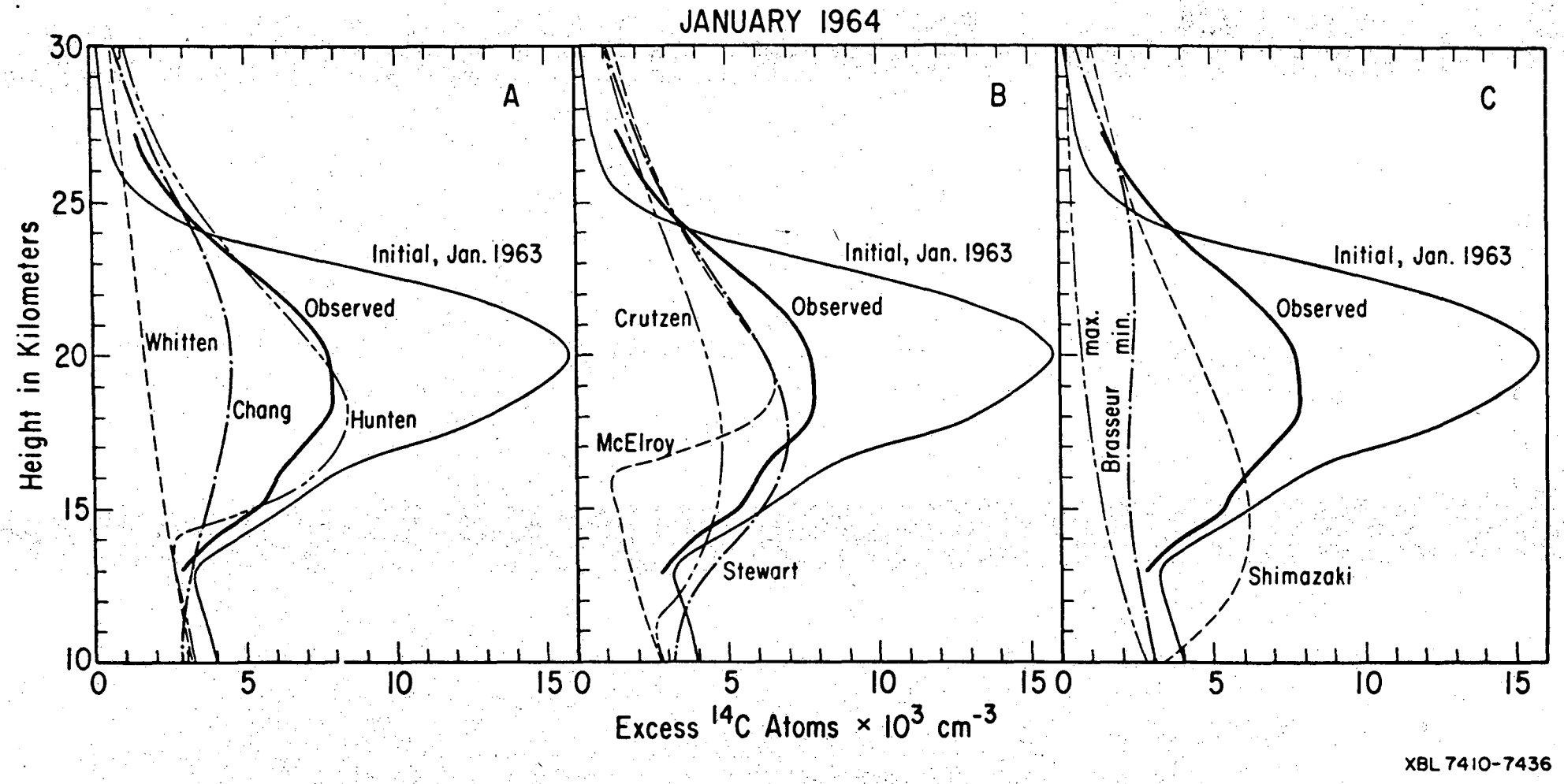
JANUARY 1964
A
B
C
Initial, Jan. 1963
Observed
Whitten
Chang
Hunten
Crutzen
McElroy
Stewart
max.
min.
Brasseur
Shimazaki
Height in Kilometers
Excess ^{14}C Atoms × 10^3 cm^{-3}
XBL 7410-7436

FIGURE 9

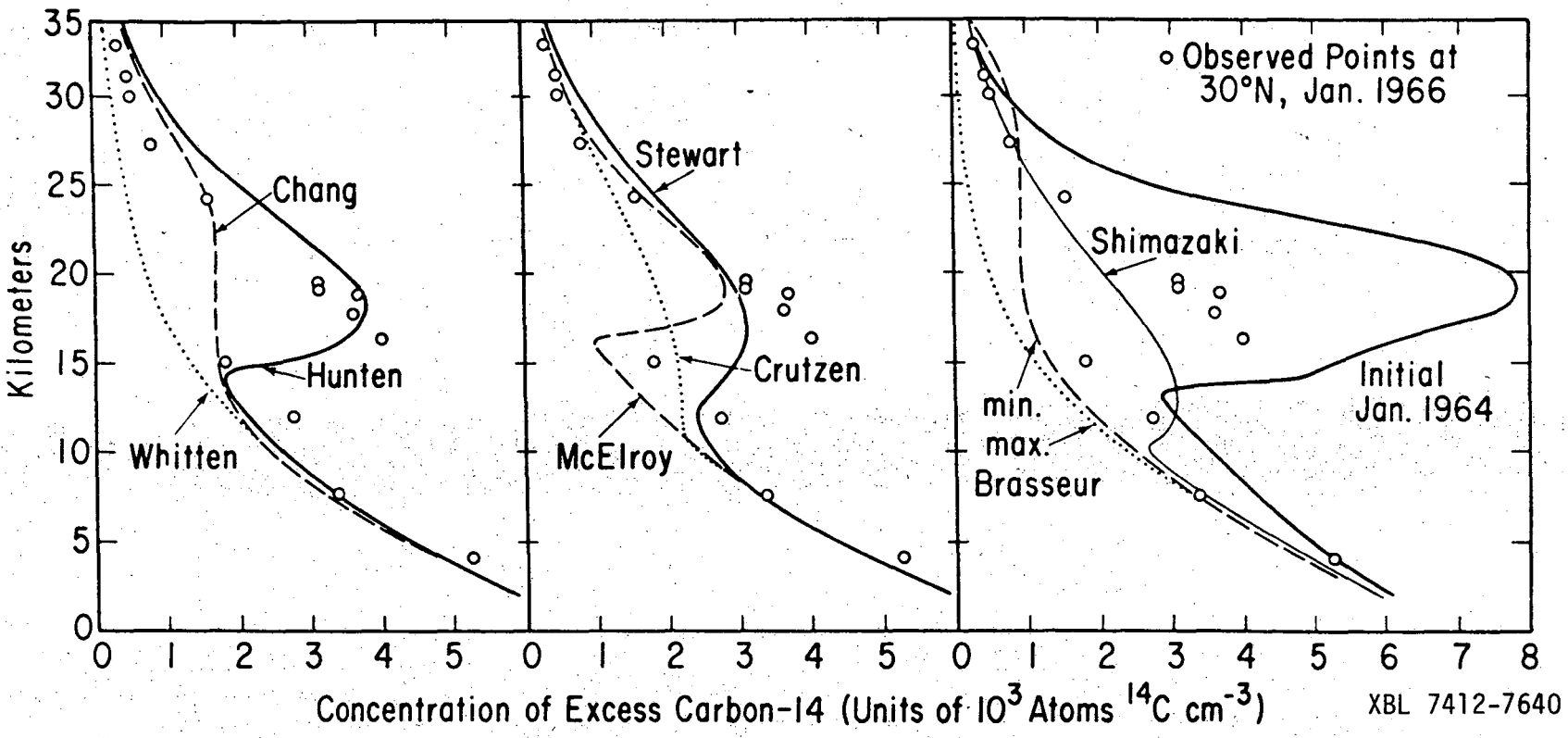

FIGURE 10

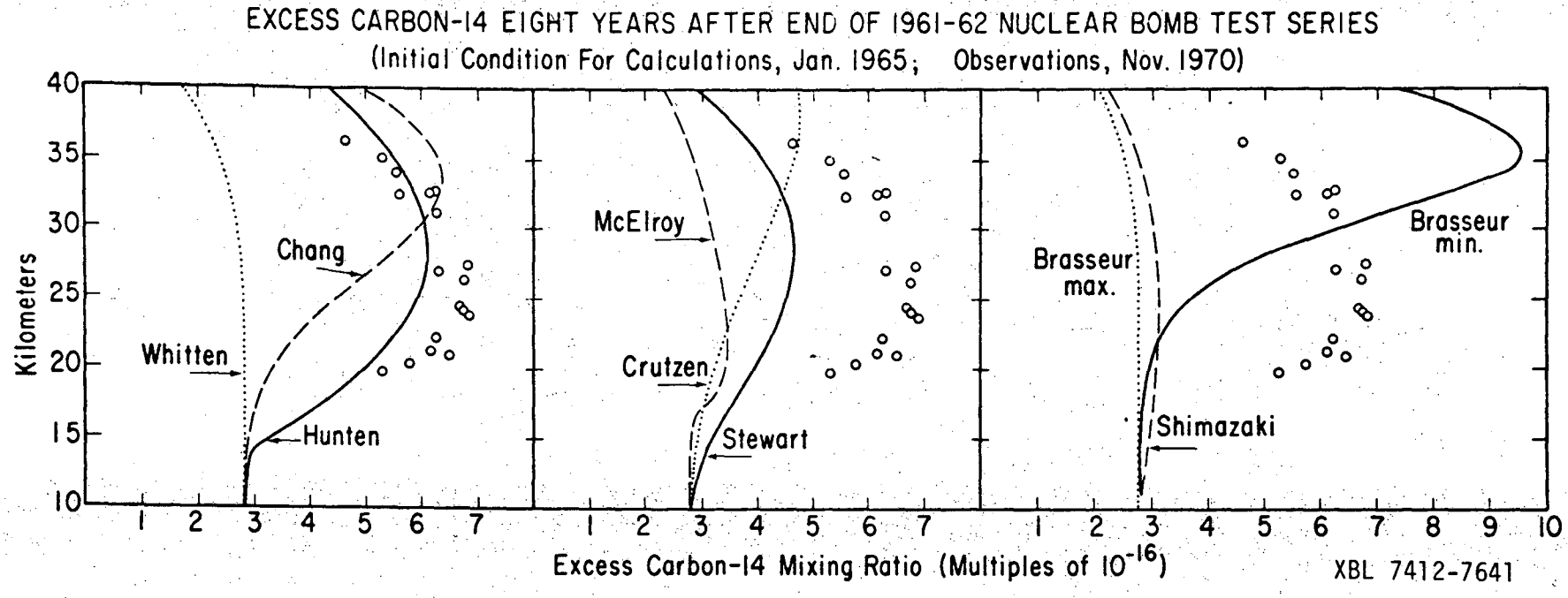
EXCESS CARBON-14 EIGHT YEARS AFTER END OF 1961-62 NUCLEAR BOMB TEST SERIES
(Initial Condition For Calculations, Jan. 1965; Observations, Nov. 1970)
Kilometers
40
35
30
25
20
15
10
Chang
Whitten
Hunten
McElroy
Crutzen
Stewart
Brasseur max.
Brasseur min.
Shimazaki
1 2 3 4 5 6 7
1 2 3 4 5 6 7
1 2 3 4 5 6 7 8 9 10
Excess Carbon-14 Mixing Ratio (Multiples of 10^{-16})
XBL 7412-7641

FIGURE 11

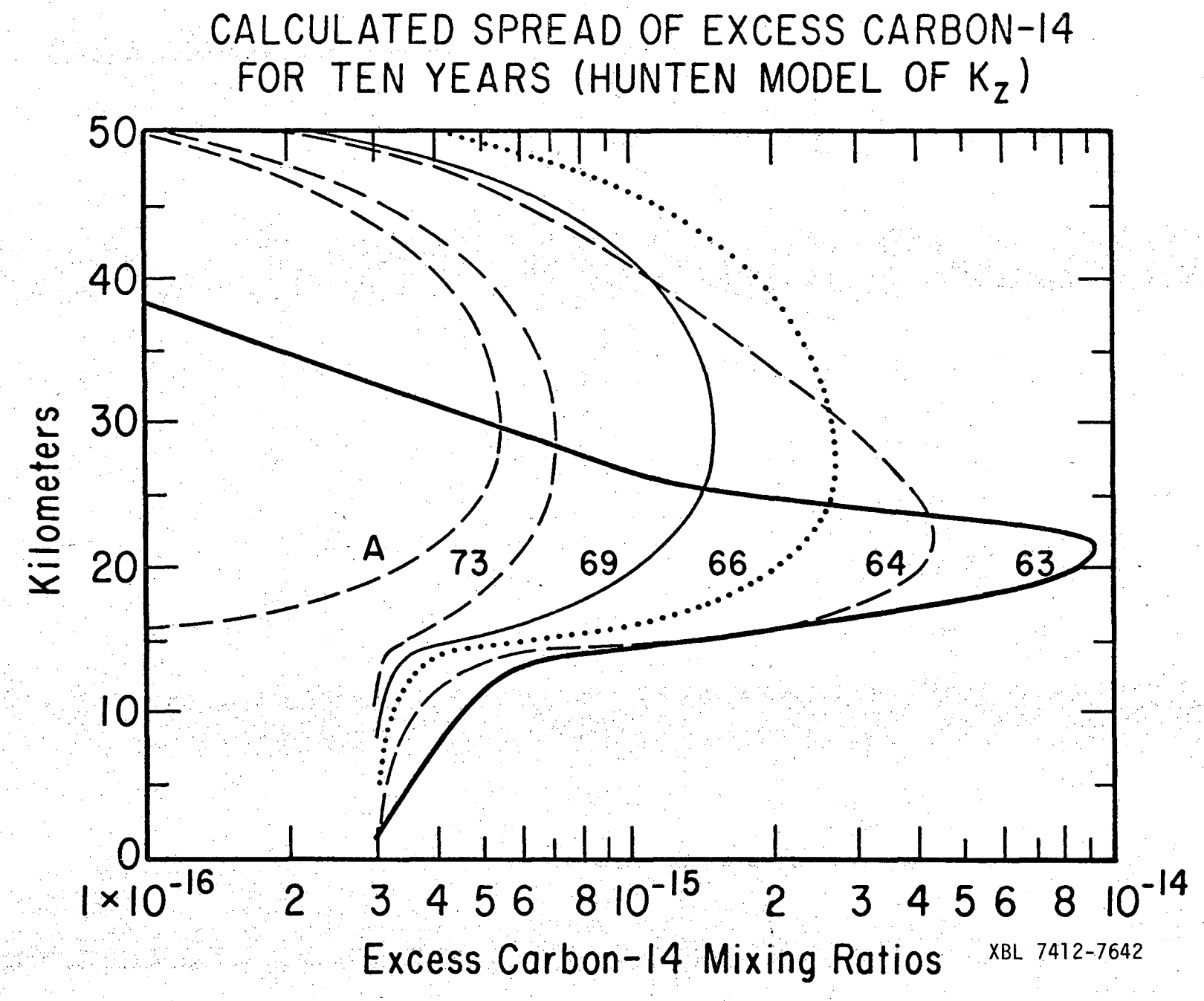

FIGURE 12

APPENDIX

Tables A1, A2, A3, A4, A5, A6

TABLE A1

VERTICAL EDDY DIFFUSION FUNCTION K_z

(IN UNITS OF 10^3 cm^2 sec^{-1})

Kilometers

1	2	3	4	5	6	7	8	9	10
11	12	13	14	15	16	17	18	19	20
21	22	23	24	25	26	27	28	29	30
31	32	33	34	35	36	37	38	39	40
41	42	43	44	45	46	47	48	49	50

Hunten

100.	100.	100.	100.	100.	100.	100.	100.	100.	30.
30.	30.	30.	2.3	2.3	2.7	3.0	3.3	3.7	4.2
4.5	5.2	5.6	6.4	7.2	8.0	9.0	10.	11.	12.
13.	15.	16.	18.	20.	22.	24.	28.	30.	34.
38.	41.	47.	52.	59.	63.	72.	80.	90.	100.

Chang

300.	300.	300.	300.	300.	300.	300.	300.	300.	300.
23.	18.	15.	12.	11.	9.7	8.6	7.4	6.6	6.0
5.3	5.0	4.5	4.2	4.0	3.9	3.7	3.7	3.7	3.7
3.8	3.9	4.0	4.2	4.5	5.0	5.4	6.1	7.0	8.0
9.2	11.	13.	15.	18.	22.	26.	33.	42.	54.

Stewart

300.	300.	300.	300.	270.	220.	150.	90.	42.	23.
13.	8.2	6.0	5.1	5.0	5.1	5.2	5.4	5.6	6.0
6.2	6.6	7.0	7.3	7.8	8.2	8.9	9.1	9.9	11.
12.	13.	14.	15.	16.	18.	20.	22.	26.	30.
33.	40.	45.	56.	66.	76.	93.	120.	140.	160.

Whitten

100.	100.	100.	100.	100.	100.	100.	100.	100.	44.
42.	40.	38.	35.	34.	32.	31.	28.	27.	26.
25.	23.	22.	21.	20.	19.	18.	17.	16.	15.
15.	14.	14.	14.	14.	14.	15.	16.	17.	18.
20.	22.	25.	3.0	35.	42.	56.	75.	100.	130.

Shimazaki

100.	100.	100.	100.	100.	100.	100.	100.	100.	6.4
7.0	7.5	8.1	8.9	9.2	10.	11.	12.	13.	14.
14.	15.	16.	17.	18.	20.	23.	24.	25.	27.
29.	31.	33.	35.	39.	42.	44.	48.	51.	55.
6.0	63.	69.	73.	80.	85.	91.	99.	110.	120.

McElroy

300.	300.	300.	300.	300.	300.	300.	300.	300.	300.
300.	300.	300.	300.	300.	2.0	2.0	2.0	4.0	7.0
9.0	12.	15.	19.	22.	25.	30.	35.	40.	45.
52.	59.	65.	7.2	81.	90.	9.9	110.	120.	130.
140.	150.	160.	170.	180.	200.	220.	230.	240.	260.

Kilometers

1	2	3	4	5	6	7	8	9	10
11	12	13	14	15	16	17	18	19	20
21	22	23	24	25	26	27	28	29	30
31	32	33	34	35	36	37	38	39	40
41	42	43	44	45	46	47	48	49	50

Crutzen

300.	300.	300.	300.	300.	300.	300.	300.	300.	300.
10.	10.	10.	10.	10.	10.	10.	10.	10.	10.
10.	10.	10.	10.	10.	10.	10.	10.	10.	10.
10.	10.	10.	10.	10.	10.	10.	10.	10.	10.
10.	10.	10.	10.	10.	10.	10.	10.	10.	10.

Brass Min.

190.	180.	170.	150.	140.	130.	120.	98.	82.	70.
58.	45.	38.	31.	25.	21.	18.	14.	12.	10.
8.1	6.5	5.5	4.3	3.4	2.8	2.3	1.9	1.5	1.3
1.1	.80	.75	.62	.54	.51	.51	.52	.54	.58
.65	.74	.83	.95	1.1	1.2	1.4	1.7	2.0	2.2

Brass Max.

190.	180.	170.	160.	150.	145.	140.	135.	130.	127.
124.	120.	115.	110.	98.	91.	84.	78.	71.	64.
60.	53.	48.	43.	38.	34.	30.	26.	23.	22.
20.	17.	15.	14.5	14.	14.	14.	14.5	15.	16.
17.	18.	21.	22.	23.	25.	28.	32.	34.	38.

TABLE A2.A

MIXING RATIOS (V/V) OF EXCESS CARBON-14 AT 30°N

(MULTIPLES OF 10^{-16}), BASED ON DIRECTLY OBSERVED LOCAL VALUES.

KM	1/63	4/63	7/63	10/63	1/64	1/65
36						
35						
34						
33			20.6	18.5	16.9	12.1
32	7.58	9.55				
30			24.0	23.8	19.2	21.4
27		20.2	22.1	26.7	20.2	18.0
26	9.60					
25	10.0	33.6		44.6		
24		35.5	39.8		30.7	22.4
22						
21						
20	77.1	59.4	46.8	55.1	40.4	24.9
19	73.0		43.8			18.3
18	55.7	40.2	33.6	30.9	31.7	14.3
15	20.8	9.84	5.23	8.48	7.54	4.85
12	5.81	11.3	3.02	3.36	3.98	3.93
8	2.92	3.79	3.12	2.98	3.60	3.17
4	2.98	3.12	2.93	2.93	3.65	2.93
0		2.10	2.91	2.77	2.84	2.75

TABLE A2.B

CARBON-14 MIXING RATIOS α AS OBSERVED BY BALLOON AS VARIOUS LATITUDES AND HEIGHTS (MULTIPLES OF 10^{-16}), JANUARY 1966

9°N		30°N		70°N	
km	α	km	α	km	α
4.5	2.84	4.5	3.18	1.0	3.18
8.5	2.80	8.3	2.99	4.3	3.08
12.0	2.99	11.8	3.42	7.5	3.18
14.8	3.13	15.0	4.34	11.9	7.04
18.0	3.90	16.2	11.7	15.0	13.0
19.0	4.58	17.8	13.4	17.8	16.1
19.5	4.63	18.8	17.1	18.5	15.3
		19.0	14.2	18.8	19.4
		19.5	15.0	19.2	18.4
		24.0	16.7		
		27.2	14.1		
		30.0	14.1		
		31.0	15.8		
		32.8	14.3		

TABLE A2.C

CARBON-14 MIXING RATIOS α OBSERVED BY BALLOON AND CONTOUR LINES AS INFERRED FROM BALLOON PLUS AIRCRAFT SAMPLING (MULTIPLES OF 10^{-16}). NOVEMBER 1970.

9°N	
km	α
20.8	3.71
21.0	3.86
21.4	4.34
22.0	4.82
23.0	5.30
23.7	5.78
27.2	5.35
30.6	5.30
31.5	5.11

34°S	
km	α
20.0	5.78
20.9	5.74
21.1	6.17
21.7	6.27
23.9	6.27
24.2	6.51
27.0	6.46
27.2	6.27
27.3	5.78
32.3	5.78

30°N	
km	α
19.6	5.30
20.3	5.78
21.0	6.51
21.2	6.17
22.2	6.27
23.9	6.84
24.3	6.75
24.4	6.70
26.5	6.75
27.2	6.31
27.6	6.84
31.2	6.27
32.5	5.59
32.8	6.17
33.0	6.27
34.0	5.78
35.5	5.30
36.3	4.63

42°N	
km	α
19.6	5.78
20.9	6.03
21.3	6.27
23.3	6.75
24.0	6.89
27.2	6.75
27.4	6.65
30.8	6.46
31.5	6.27
36.0	6.03

65°N	
km	α
20.3	6.27
22.3	6.75
24.0	6.70
26.9	6.80
27.0	6.75
30.0	6.27
31.0	5.78

TABLE A3.A

CONCENTRATION OF EXCESS CARBON-14 (10^3 MOLECULES CM^{-3})

January 1963

KM.	80°N	70°N	60°N	50°N	40°N	30°N	20°N	10°N	0°N	10°S	20°S	30°S
29								0.3	0.3	0.3		
28							0.4	0.5	0.5	0.5	0.4	
27						0.4	0.6	0.6	0.6	0.6	0.6	0.4
26					0.6	0.6	0.8	0.8	0.8	0.8	0.8	0.6
25				0.8	0.8	0.8	1.0	1.4	1.2	1.0	0.8	0.8
24		0.9	1.0	1.2	1.0	1.4	2.8	3.0	1.6	1.2	1.0	0.8
23	1.2	1.2	1.4	1.6	2.0	5.6	6.4	4.2	1.8	1.2	1.0	1.0
22	1.8	1.8	2.8	4.4	9.4	11.6	10.4	4.4	1.8	1.4	1.2	1.0
21	3.8	5.6	10.2	12.0	15.8	14.8	12.2	4.2	1.8	1.6	1.2	1.0
20	12.6	13.4	16.4	18.4	18.2	16.4	12.6	3.6	1.6	1.4	1.2	1.2
19	19.4	20.6	20.8	21.4	18.6	16.0	11.4	3.0	1.4	1.4	1.4	1.2
18	25.0	25.2	24.8	22.8	17.0	14.8	6.8	2.2	1.2	1.2	1.4	1.2
17	30.4	28.6	27.0	21.2	15.2	12.2	5.8	1.4	1.2	1.0	1.4	1.2
16	33.6	30.6	25.0	19.2	13.0	9.2	5.0	1.2	1.0	1.0	1.4	1.4
15	32.8	28.2	22.0	16.4	10.8	7.4	4.2	1.0	0.8	0.8	1.2	1.2
14	28.8	23.8	18.0	12.0	8.8	6.4	3.6				1.2	1.2

TABLE A3.A

CONCENTRATION OF EXCESS CARBON-14 (10^3 MOLECULES CM^{-3})

(Continued)

January 1963

KM.	80°N	70°N	60°N	50°N	40°N	30°N	20°N	10°N	0°N	10°S	20°S	30°S
13	21.4	16.0	12.6	9.2	6.2	5.4						1.2
12	14.0	11.6	9.8	6.2	3.6							
11	11.4	9.8	4.6	3.4								
10	9.8	7.6	4.0									
9	8.0	4.2										
8	4.4											

TABLE A3.B

April 1963

KM.	80°N	70°N	60°N	50°N	40°N	30°N	20°N	10°N	0°	10°S	20°S	30°S
29								0.7	0.7	0.6		
28							1.0	0.8	1.0	0.6	0.4	
27						1.1	1.4	1.4	1.3	0.6	0.4	0.4
26					1.3	1.6	2.0	2.4	1.7	0.6	0.4	0.4
25				1.7	2.0	2.2	3.0	4.0	2.2	0.6	0.5	0.4
24			2.2	2.6	3.2	3.6	4.6	5.2	2.6	0.7	0.5	0.5
23		3.0	3.4	3.8	4.8	5.4	7.2	6.0	2.8	0.9	0.8	0.5
22	4.2	5.0	5.4	6.2	7.2	9.4	9.2	5.2	2.5	1.3	1.1	0.8
21	6.4	7.6	7.8	9.0	11.0	9.8	9.4	3.8	2.2	1.5	1.5	1.0
20	9.6	10.6	11.0	12.8	13.8	12.8	8.0	3.5	2.2	1.5	1.6	1.3
19	12.2	14.2	16.8	16.4	15.2	11.6	5.2	3.0	1.9	1.4	1.4	1.2
18	16.2	18.4	21.0	18.0	14.4	9.8	4.0	2.0	1.6	1.3	1.3	1.2
17	21.4	22.6	21.0	17.0	12.8	8.2	2.6	1.6	1.4	1.0	1.1	1.1
16	24.4	22.8	19.2	15.4	11.6	5.8	2.2	1.2	1.0	0.8	1.0	1.0
15	24.0	21.4	18.2	14.0	12.6	4.6	2.0	1.0	0.8	0.8	1.0	1.0
14	23.2	20.2	17.6	15.4	13.8	6.8	2.4				0.9	0.9
13	22.2	19.4	17.0	15.6	13.6	8.2						0.9

TABLE A3.B

April 1963 (Continued)

KM.	80°N	70°N	60°N	50°N	40°N	30°N	20°N	10°N	0°N	10°S	20°S	30°S
12	21.4	18.4	16.4	9.2	6.8							
11	20.0	16.6	8.4	5.2								
10	11.8	8.4	5.8									
9	8.2	6.4										
8	6.6											

TABLE A3.C

July 1963

KM.	80°N	70°N	60°N	50°N	40°N	30°N	20°N	10°N	0°	10°S	20°S	30°S
29								1.0	1.0	1.0		
28							1.3	1.3	1.2	1.2		
27						1.6	1.7	1.6	1.4	1.4		
26					2.0	2.1	2.2	2.0	1.6	1.7		
25		2.2	2.0	2.4	2.7	3.0	3.2	2.7	2.0	2.1		
24	2.7	2.8	3.2	3.4	3.8	4.2	4.4	3.6	2.5	2.4	1.0	
23	3.3	3.6	4.2	4.4	5.2	5.9	6.0	4.4	3.0	2.6	1.1	
22	4.8	4.8	5.6	6.2	7.2	8.3	7.0	5.0	3.6	2.7	1.2	
21	6.6	6.8	7.6	9.0	10.6	10.2	7.3	5.1	4.3	2.6	1.4	
20	8.8	9.8	11.0	12.4	12.0	10.7	7.4	5.0	4.5	2.4	1.5	
19	12.8	13.0	14.8	13.2	12.4	9.5	7.7	4.8	4.0	2.1	1.6	
18	15.8	15.8	16.8	13.3	11.6	9.2	8.2	4.3	3.1	1.8	1.5	1.4
17	18.4	17.6	15.2	10.4	8.8	9.8	6.4	3.6	1.9	1.5	1.2	1.3
16	20.2	17.4	11.4	7.2	7.2	7.8	3.8	1.8	1.3	1.3	1.2	
15	17.8	14.2	9.4	6.6	6.0	3.3	1.7	1.4	1.3	1.2		
14	17.0	13.2	10.2	7.3	5.2	2.6	1.8					
13	15.6	14.1	11.8	8.6	4.4	2.1						

TABLE A3.C

July 1963 (Continued)

KM.	80°N	70°N	60°N	50°N	40°N	30°N	20°N	10°N	0°	10°S	20°S	30°S
12	15.4	14.4	12.8	7.9	3.8							
11	15.8	14.8	11.6	6.4								
10	16.0	13.0	8.2									
9	11.4	9.2										
8	8.0											

TABLE A3.D

October 1963

KM.	80°N	70°N	60°N	50°N	40°N	30°N	20°N	10°N	0°	10°S	20°S	30°S
29								1.0	0.9	0.9		
28							1.4	1.3	1.1	1.0	0.4	
27						1.6	1.8	1.7	1.4	1.1	0.5	0.4
26					2.2	2.3	2.6	2.0	1.6	1.3	0.7	0.5
25				2.8	3.2	3.2	3.6	2.3	2.0	1.6	0.8	0.6
24			3.7	3.8	4.2	4.4	4.6	3.1	2.4	1.8	0.9	0.7
23		4.6	5.0	5.2	5.6	5.8	5.7	3.8	2.8	2.0	1.1	0.9
22	5.9	6.0	5.9	6.6	7.2	7.9	6.8	4.4	3.3	2.2	1.2	1.0
21	7.4	7.5	7.9	8.2	9.1	9.6	7.7	4.9	3.6	2.2	1.4	1.2
20	9.4	9.7	10.3	10.5	10.8	9.8	7.8	5.1	3.7	2.2	1.7	1.4
19	12.0	12.1	12.4	11.9	11.4	9.0	7.2	5.0	3.2	2.2	1.9	1.7
18	14.4	14.2	13.6	12.6	10.4	8.1	5.6	4.0	2.5	2.2	1.9	1.7
17	16.0	15.5	14.4	12.9	5.4	4.5	3.9	2.8	2.2	2.0	2.2	1.6
16	17.2	15.2	14.5	13.3	5.0	4.0	3.0	1.6	1.6	1.6	1.6	1.5
15	15.2	12.8	13.0	14.1	4.8	3.6	1.8	1.4	1.4	1.4	1.4	1.4
14	14.0	10.9	8.9	8.0	4.5	3.1	1.7				1.5	1.5
13	11.2	9.3	8.0	6.5	4.2	2.3						

TABLE A3.D

October 1963 (Continued)

KM.	80°N	70°N	60°N	50°N	40°N	30°N	20°N	10°N	0°	10°S	20°S	30°S
12	10.2	8.6	7.6	3.4	3.6							
11	9.7	8.4	7.2	4.9								
10	9.0	8.0	6.3									
9	7.9	6.4										
8	6.8											

TABLE A3.E

January 1964

KM.	80°N	70°N	60°N	50°N	40°N	30°N	20°N	10°N	0°	10°S	20°S	30°S
29								0.9	0.9	0.9		
28							1.0	1.0	0.9	0.9	0.8	
27						1.2	1.2	1.1	1.0	1.0	0.8	0.7
26					1.6	1.6	1.8	1.2	1.3	1.0	0.8	0.8
25				2.1	2.2	2.4	2.4	1.5	1.6	1.2	0.9	0.8
24			2.6	2.8	3.2	3.2	3.4	2.0	1.7	1.4	0.9	0.9
23		3.2	3.6	3.8	4.4	4.6	4.6	3.4	1.8	1.6	1.0	0.9
22	4.2	4.4	4.8	5.2	5.6	6.0	5.6	3.8	1.9	1.6	1.1	1.0
21	5.4	6.0	6.6	7.0	7.8	7.4	6.4	3.6	1.9	1.6	1.2	1.1
20	7.2	7.6	8.2	8.6	8.6	8.2	6.6	3.4	1.8	1.6	1.1	1.1
19	9.0	9.0	10.0	9.4	9.4	8.8	6.4	2.8	1.8	1.4	1.1	1.0
18	11.4	10.8	11.0	10.2	10.0	8.2	5.4	2.4	1.8	1.4	1.0	1.0
17	13.0	12.0	11.2	11.0	9.6	7.2	3.2	2.0	1.7	1.4	1.0	1.0
16	14.2	12.2	9.2	10.2	9.0	4.8	2.3	1.7	1.6	1.4	1.2	1.1
15	14.8	13.0	11.4	6.8	9.0	3.4	1.9	1.6	1.6	1.4	1.3	1.2
14	15.2	13.8	12.6	7.8	10.4	3.4	1.8				1.5	1.4

TABLE A3.E

January 1964 (Continued)

KM.	80°N	70°N	60°N	50°N	40°N	30°N	20°N	10°N	0°	10°S	20°S	30°S
13	14.6	13.0	11.6	8.2	8.4	2.6						
12	13.0	12.0	8.8	2.4	4.0							
11	11.2	10.4	6.2	3.0								
10	9.6	7.0	4.4									
9	7.6	5.4										
8	5.8											

TABLE A3.1

January 1965 (Continued)

KM.	80°N	70°N	60°N	50°N	40°N	30°N	20°N	10°N	0°	10°S	20°S	30°S
14	6.0	6.0	5 .2	2.6	2.2	1.6	1.2				1.0	1.0
13	5.7	4.8	4.0	2.5	2.1	1.7						1.0
12	5.4	4.4	3.6	2.4	2.2							
11	5.0	4.0	3.4	2.6								
10	4.6	3.8	3.2									
9	4.2	3.4										
8	4,0											

TABLE A3.F

January 1965

KM.	80°N	70°N	60°N	50°N	40°N	30°N	20°N	10°N	0°	10°S	20°S	30°S
29								0.9	0.5	0.5		
28							1.2	1.0	0.6	0.6	0.5	
27						1.6	1.4	1.2	0.8	0.8	0.6	0.7
26					1.5	1.8	1.8	1.4	1.0	1.0	0.8	0.8
25				2.0	1.8	2.1	2.0	1.7	1.2	1.2	1.0	0.9
24			2.0	2.2	2.2	2.4	2.4	2.0	1.4	1.4	1.2	1.0
23		2.4	2.4	2.7	2.6	2.8	2.8	2.4	1.7	1.7	1.5	1.2
22	3.0	2.8	2.9	3.2	3.2	3.4	3.2	2.6	2.0	2.0	1.8	1.4
21	3.4	3.3	3.4	3.6	3.8	3.9	3.8	2.7	2.4	2.2	2.0	1.7
20	4.0	3.8	4.0	4.2	4.4	4.4	3.8	2.6	2.6	2.4	2.2	1.9
19	4.6	4.6	4.8	5.2	5.0	4.4	3.4	2.6	2.3	2.2	2.3	2.0
18	5.4	5.4	5.6	5.8	5.0	3.8	2.6	1.2	1.4	1.4	1.8	1.8
17	6.0	5.8	5.9	5.4	4.4	3.0	1.6	1.0	0.8	0.9	1.3	1.6
16	6.3	6.0	5.8	5.2	3.4	1.8	1.4	1.0	0.9	1.0	1.0	1.4
15	6.3	6.0	5.8	4.0	2.6	1.4	1.2	1.1	1.1	1.2	1.0	1.2

TABLE A4

RELATIVE MIXING RATIO* OF STRONTIUM-90 AT 30°N

April 1963		July 1963		October 1963		Jan. 1964		Jan. 1965		Jan. 1966	
KM	$^{90}S_R$	KM	$^{90}S_R$	KM	$^{90}S_R$	KM	$^{90}S_R$	KM	$^{90}S_R$	KM	$^{90}S_R$
30.3	200	29.0	300	32.0	200	29.5	100	30.3	30	32.5	10
28.0	500	28.0	400	28.5	300	26.5	200	26.8	50	29.8	20
24.3	1000	26.5	500	26.5	500	25.2	300	25.2	100	28.2	30
23.2	1500	23.9	1000	23.7	1000	23.6	500	21.8	200	27.0	40
21.8	1700	22.8	1500	21.9	1200	22.4	800	21.4	300	26.0	50
19.3	1700	21.8	1700	21.2	1500	21.6	900	20.9	350	24.6	100
18.5	1500	19.2	1700	19.4	1500	20.6	1000	19.2	350	22.2	150
17.7	1000	18.6	1500	19.1	1200	19.2	1000	17.9	300	20.0	150
16.2	500	17.8	1000	18.5	1000	18.7	900	16.7	200	18.3	130
14.0	200	16.5	500	17.2	500	18.3	800	16.2	100	17.8	100
10.8	100	16.0	200	16.2	300	17.2	500	15.8	50	17.0	50
9.5	50	15.5	100	15.8	200	16.2	300	14.0	10	12.0	10
7.3	26	14.9	50	15.6	100	15.7	200				
6.0	14	14.1	10	15.2	50	13.5	100				
4.5	7			14.0	10	12.0	50				
						10.5	22				

*In Units of Disintegrations per Minute per 1000 Cubic Feet of Standard Air.

TABLE A.5

AVERAGE CONCENTRATION OF EXCESS CARBON-14 AT 30°N

(UNITS OF 10^3 ATOMS CM^{-3})

KM	1/63	4/63	7/63	10/63	1/64	1/65
27	0.619	1.389	2.091	2.146	1.587	1.480
26	0.892	2.080	2.526	2.845	2.056	1.704
25	1.728	3.118	3.426	3.754	2.807	2.070
24	3.692	4.659	4.713	4.870	3.700	2.403
23	7.757	6.775	6.458	6.190	4.819	2.850
22	11.97	9.911	8.710	7.753	6.113	3.360
21	14.65	11.95	9.985	8.924	7.134	3.891
20	15.72	12.63	10.09	9.370	7.709	4.311
19	14.84	11.47	9.070	9.125	7.855	4.282
18	13.10	10.10	8.072	8.023	7.765	4.031
17	10.16	9.109	7.952	6.732	6.888	3.351
16	7.783	8.449	7.306	5.197	6.000	2.281
15	6.257	7.859	6.165	4.504	5.400	1.965
14	4.596	6.001	4.777	3.716	3.860	1.903
13	3.257	4.473	3.732	3.176	2.874	1.941

TABLE A.6

MIXING RATIOS (V/V) OF EXCESS CARBON-14 AT 30°N

(MULTIPLES OF 10^{-16}), BASED ON AVERAGE VALUES FROM TABLE A5.

KM	1/63	4/63	7/63	10/63	1/64	1/65
27	10.235	22.966	34.573	35.483	26.240	24.471
26	12.578	29.329	35.618	40.116	28.990	24.027
25	20.739	37.422	41.119	45.055	33.685	24.844
24	38.386	48.440	49.002	50.634	38.470	24.984
23	67.021	58.536	55.797	53.482	41.636	24.624
22	87.692	72.608	63.810	56.799	44.784	24.615
21	90.944	74.224	62.019	55.429	44.311	24.168
20	82.824	66.544	53.161	49.368	40.616	22.713
19	66.398	51.320	40.582	40.828	35.145	19.159
18	49.848	38.432	30.715	30.529	29.547	15.339
17	32.966	29.555	25.801	21.843	22.349	10.873
16	21.619	23.469	20.294	14.436	16.667	6.336
15	14.933	18.757	14.714	10.749	12.888	4.690
14	9.476	12.373	9.849	7.662	7.959	3.924
13	5.837	8.016	6.688	5.692	5.151	3.478

MIXING RATIOS (V/V) OF EXCESS CARBON-14 AT 30°N

(MULTIPLES OF 10^{-16})

Height	Jan. 1963		April 1963		July 1963		Oct. 1963		Jan. 1964		Jan. 1965		Dec. 1970
KM.	Local	Ave.	Local	Ave.	Local	Ave.	Local	Ave.	Local	Ave.	Local	Ave.	Local
36													4.6
35													5.3
34													5.8
33					20.6		18.5		16.9		12.1		6.0
32	7.58		9.55										6.2
30					24.0		23.8		19.2		21.4		
27		12.4	20.2	24.2	22.1	38.0	26.7	38.2	20.2	30.2	18.0	26.6	6.5
26	9.60	14.5		29.2		38.4		41.8		31.4		26.2	6.7
25	10.0	20.6	33.6	35.6		42.6	44.6	45.8		34.8		27.4	
24		34.0	35.5	44.6	39.8	48.4		49.8	30.7	38.0	22.4	27.2	6.7
23		60.8		54.4		55.6		53.2		41.2		27.4	
22		79.6		67.4		62.4		56.2		44.0		27.6	6.3
21		82.8		68.8	66.4	60.6		54.8		43.4		27.4	6.3
20	77.1	75.6	59.4	62.6	46.8	53.0	55.1	49.6	40.4	39.8	24.9	26.0	5.8
19	78.0	61.2		48.4	43.8	41.6		41.6		34.2	18.3	22.6	5.3
18	55.7	46.6	40.2	36.4	33.6	32.0	30.9	31.8	31.7	28.6	14.3	18.4	
17		31.4		27.8		26.6		23.2		21.8		13.2	
16		21.0		21.8		20.4		15.5		16.4		7.62	

MIXING RATIOS (V/V) OF EXCESS CARBON-14 AT 30°N

(MULTIPLES OF 10^{-16}) (Continued)

Height	Jan. 1963		April 1963		July 1963		Oct. 1963		Jan. 1964		Jan. 1965		Dec. 1970
KM.	Local	Ave.	Local	Ave.	Local	Ave.	Local	Ave.	Local	Ave.	Local	Ave.	Local
15	20.8	14.7	9.84	17.6	5.23	14.2	8.48	11.5	7.54	13.0	4.85	5.38	
14		9.62		12.0		9.74		8.22		8.56		4.52	
13		6.22		7.94		7.00		6.34		6.00		4.10	
12	5.81		11.3		3.02		3.36		3.98		3.93		
8	2.92		3.79		3.12		2.98		3.60		3.17		
4	2.98		3.12		2.93		2.93		3.65		2.93		
0			2.10		2.91		2.77		2.84		2.75		

TECHNICAL INFORMATION DIVISION
LAWRENCE BERKELEY LABORATORY
UNIVERSITY OF CALIFORNIA
BERKELEY, CALIFORNIA 94720